Table 1. Clinical characteristics of patients with MF

Patient no.	Age, sex	Duration (mo)	Clinical stage	Tumor-node-metastasis-blood classification, stage	sIL-2R (units/mL)	LDH (IU/L)	CCR10 in PBMC (%)	Serum CTACK/CCL27 (pg/mL)
1	72, M	31	Patch	$T_1N_0M_0B_0$, stage IA	243	154	0.55	600
2	66, M	430	Patch	$T_1N_0M_0B_0$, stage IA	372	194	5.19	630
3	36, F	240	Patch	$T_{2a}N_0M_0B_0$, stage IB	549	153	3.02	760
4	41, F	168	Patch	$T_{2a}N_0M_0B_0$, stage IB	262	151	1.29	660
5	67, M	35	Patch	$T_1N_0M_0B_0$, stage IA	357	200	3.36	620
6	67, M	10	Plaque	$T_{2b}N_0M_0B_0$, stage IIB	1,273	273	2.99	1,560
7	68, F	580	Plaque	$T_{2b}N_0M_0B_0$, stage IIB	796	191	0.96	910
8	50, M	9	Plaque	$T_{2b}N_0M_0B_0$, stage IIB	408	195	1.76	1,510
9	52, F	24	Plaque	$T_{2b}N_0M_0B_0$, stage IIB	425	192	4.58	1,650
10	87, F	270	Plaque	$T_{2b}N_3M_0B_0$, stage IVA	658	220	1.52	1,320
11	37, F	184	Plaque	$T_{2b}N_1M_0B_0$, stage IIB	<198	198	0.38	920
12	61, M	170	Plaque	$T_{2b}N_0M_0B_0$, stage IIB	399	154	1.08	920
13	60, F	75	Plaque	$T_{2b}N_0M_0B_0$, stage IIB	253	146	0.78	1,040
14	82, F	240	Plaque	$T_{2b}N_0M_0B_0$, stage IIB	223	173	2.33	760
15	80, F	128	Plaque	$T_{2a}N_0M_0B_0$, stage IB	1,301	201	0.45	680
16	49, M	26	Tumor	$T_3N_0M_0B_0$, stage IIIA	554	146	3.39	1,010
17	68, M	82	Tumor	$T_3N_0M_0B_0$, stage IIIA	813	202	5.3	1,500
18	60, F	106	Tumor	$T_3N_0M_0B_0$, stage IIIA	1,200	188	0.64	850

Patients and controls. Eighteen patients with MF (eight men and 10 women: mean age, 61.3 years old) from the Department of Dermatology at Hokkaido University Graduate School of Medicine were enrolled in this study (Table 1; Fig. 1). MF was diagnosed on the basis of clinical images, histopathologic findings from skin biopsies (all cases), and gene rearrangement analysis from skin tissue. Clinical stages were also evaluated according to the modified staging classification for CTCL proposed by Kashani-Sabet et al. (14). The evaluations of clinical images, including the clinical stages, were done by a single qualified dermatologist. Blood and serum samples were collected under proper, informed consent. In two patients at the tumor stage, tumor samples were analyzed for flow cytometry analysis. For control purposes, nine healthy volunteers and six atopic dermatitis patients who had widespread skin lesions with moderate activity were also investigated.

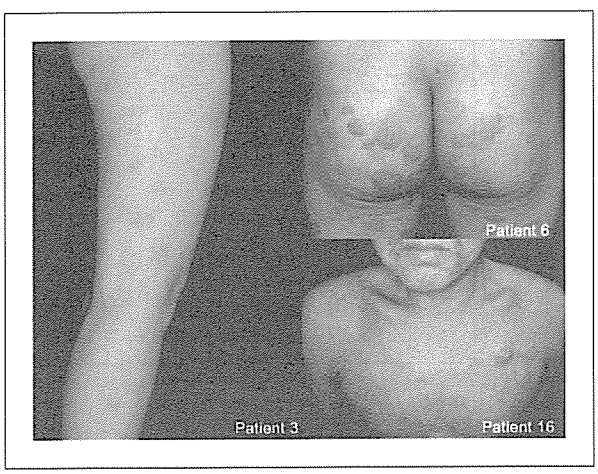

Fig. 1. Clinical images. *Patient 3,* pink-red maculae disseminated on the legs (patch stage). *Patient 6,* infiltrated erythematous plaques on the buttocks (plaque stage). *Patient 16,* poikilodermatous erythema, plaques and ulcerated nodules (tumor stage).

Flow cytometry. Peripheral blood mononuclear cells (PBMC) were isolated from heparinized venous blood by density gradient centrifugation using Ficoll. Two-color flow cytometry was done by incubation of cells (2×10^6) at 4°C. Staining for CCR10 done with monoclonal antibody against CCR10 followed by PE-labeled goat anti-mouse IgG (Rockland Immunochemical, Gilbertsville, PA) and FITC-conjugated antihuman CD4 monoclonal antibody (BD PharMingen, San Diego, CA). Cells were analyzed using a FACScan flow cytometer (Becton Dickinson, San Jose, CA), and CellQuest software (Becton Dickinson). Tumor cells were obtained from two patients' biopsy materials. The biopsy material was incubated with 200 units/mL collagenase in DMEM with 5% FCS at 37°C for 30 minutes. Suspensions were washed twice with PBS, and 50-μm filters were used to remove larger tissue fragments. Cells (1×10^6) were prepared for two-color analysis by resuspending in PBS containing 1% FCS and 1% bovine serum albumin, and flow cytometry was done as described above.

ELISA. Serum CTACK/CCL27 levels were determined using a CTACK/CCL27 ELISA kit assay in patients with MF, patients with atopic dermatitis, and healthy volunteers. We used a 96-well polystyrene microplate coated with a murine monoclonal antibody against human CTACK/CCL27. Optical densities were measured at 450 nm with a Bio-Rad Model 550 microplate reader (Bio-Rad Laboratories, Inc., Hercules, CA). The protein levels were calculated from a standard curve generated by a curve-fitting program.

Immunohistochemistry. Paraffin-embedded skin tissues from patients with MF were cut into 4-μm-thick sections. To prepare the sections for immunohistochemical analysis, they were pretreated with 3% hydrogen peroxide for 10 minutes at 4°C. They were stained with avidin-biotin peroxidase complex procedure using a Vector ABC Kit (Vector Laboratories, Burlingame, CA) according to the manufacturer's protocol. In brief, samples were treated with 10% normal goat serum for 30 minutes at room temperature followed by overnight incubation with the anti-CTACK/CCL27 monoclonal antibody or anti-CCR10 monoclonal antibody at 4°C. Positive staining was visualized with diaminobenzidine as a chromogen using a streptavidin-biotin peroxidase.

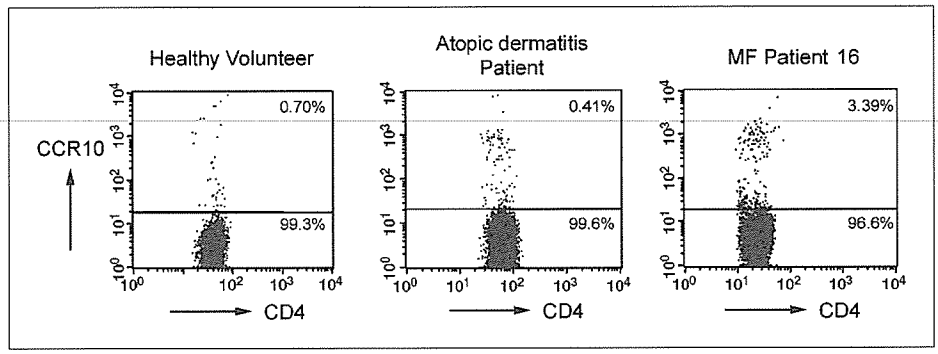

Fig. 2. PBMC CCR10 expression. PBMCs were stained with the indicated monoclonal antibodies and analyzed by flow cytometry (*left,* healthy volunteer; *middle,* atopic dermatitis patient; *right,* MF patient). The MF patient expressed more CCR10+ in circulating T cells.

Statistics. Differences between various treatments were statistically tested using Mann-Whitney *U* tests. $P < 0.05$ was considered statistically significant. Data in the figures are shown as the mean ± SE of multiple samples.

Results

Flow cytometric analysis of CCR10 expression in circulating CD4+ cells. Representative flow cytometry analyses of the surface expressions of CD4 and CCR10 in a healthy volunteer, an atopic dermatitis patient, and MF patient 16 are shown in Fig. 2. Summary of percentages of CCR10+ CD4+ cells in the CD4+ T cell population is shown in Fig. 3. The average percentages of CCR10+ cells were 0.91 ± 0.13%, 0.55 ± 0.15%, and 2.19 ± 0.39% in healthy volunteers (n = 9), patients with atopic dermatitis (n = 6) and patients with MF (n = 18), respectively. Patients with MF express significantly more CCR10+ CD4+ cells ($P < 0.05$). When classified into clinical stages of MF, the average percentages were 2.68 ± 0.82%, 1.68 ± 0.41%, and 3.11 ± 1.35% in patch stage (n = 5), plaque stage (n = 10), and tumor stage (n = 3), respectively. Also, the average percentages were 2.31 ± 0.76% (stage I, n = 6), 1.86 ± 0.49% (stage II, n = 8), and 2.71 ± 1.04% (stages III and IV, n = 4). There was no statistical correlation between CCR10 expression and the MF patient clinical stage. Immunohistochemical analysis for CCR10 in MF skin tissue also showed strong CCR10 expression in tumor cells (Fig. 4, top). Flow cytometric analysis for CCR10 in skin tissue was also investigated in skin tumor cells. CCR10 was markedly expressed in 34.03% of mononuclear cells (patient 16, tumor stage; Fig. 4, bottom). These results are consistent with a recent study (9).

Serum CTACK/CCL27 levels by ELISA. The serum CTACK/CCL27 concentrations in patients with MF were 993.6 ± 84.3 pg/mL. Conversely, those in healthy volunteers (n = 9) and atopic dermatitis patients (n = 6) were 430.6 ± 26.0 and 887.0 ± 56.9 pg/mL, respectively (Fig. 5, top). Serum CTACK/CCL27 levels were statistically elevated in patients with MF compared with normal controls ($P < 0.05$), but no statistical difference was found between patients with atopic dermatitis, in which the elevation of serum CTACK/CCL27 had been previously reported (15). Compared with each MF clinical stage, serum CTACK/CCL27 levels were 652.5 ± 28.3, 1,126.6 ± 111.7, and 1,118.7 ± 196.4 pg/mL during the patch (n = 5), plaque (n = 10), and tumor stages (n = 3), respectively. Statistically significant increases were found between the patch stage and the other two stages (Fig. 5, bottom). According to the tumor-node-metastasis classification, the average levels were 656.5 ± 23.5 (stage I, n = 6), 1,158.8 ± 125.0 (stage II, n = 8), and 1,169.0 ± 147.7 pg/mL (stages III and IV, n = 4). Patients with stage II or more advanced stages also showed a statistically higher level of serum CTACK/CCL27 than those with MF disease stage I ($P < 0.05$).

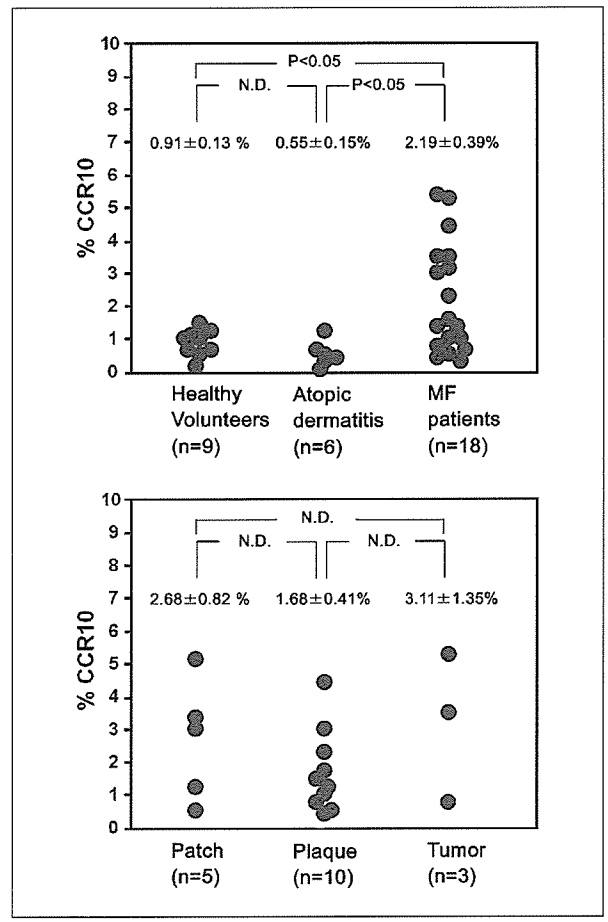

Fig. 3. CCR10 analysis using flow cytometry in PBMCs. *Top,* the percentage of CCR10+ T cells in PBMCs of MF patients were 0.55% to 5.3% (2.19 ± 0.39; average ± SE), which statistically exceeded those of healthy volunteers and patients with atopic dermatitis. *Bottom,* the expression of CCR10 was not correlated with MF clinical or disease stage.

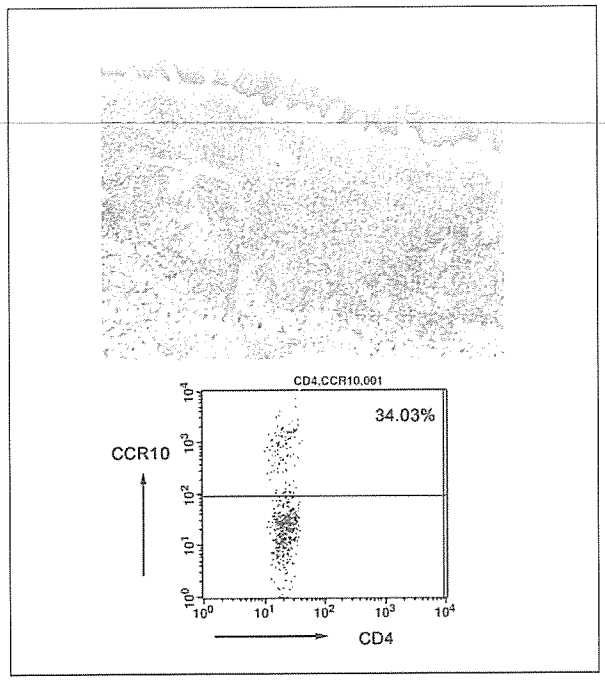

Fig. 4. CCR10 analysis in MF tumor tissues in patient 16. *Top,* marked CCR10 expression was noted in the abnormal infiltrated T cells (original magnification, ×50). *Bottom,* flow cytometric analysis also revealed increases in CCR10+ T cells within the lesional MF tissues.

Immunohistochemistry for CTACK/CCL27 in skin tissues. CTACK/CCL27 was strongly expressed in keratinocytes around both basal and suprabasal epidermal layers. CTACK/CCL27 diffusely stained the cytoplasm of keratinocytes (Fig. 6). In addition, endothelial cells of the superficial dermal plexus were stained. There was no correlation between the MF stages and extent of CTACK/CCL27 staining, or between serum CTACK/CCL27 levels and tissue expression (data not shown). Conversely, the CTACK/CCL27 expression in normal control skin was restricted to the basal cell layer (data not shown), as described previously (11).

Discussion

It has been shown that small numbers of clonal, aberrant T cells circulate in patients' peripheral blood even in early stages of MF, which is associated with the skipped expansion and micrometastasis of the MF lesions (3–5). In addition, circulating CLA+ CD4+ T cells express CCR10, a CC chemokine receptor for skin-homing function, in patients with CTCL (especially Sézary syndrome; ref. 8). Another study showed that malignant T cells in the MF lesional skin express CCR10 (9). Therefore, we speculate that CCR10 and its ligand CTACK/CCR27 play an important role in progression and skin-homing in early MF. In the present study, we have confirmed the previous findings in patients with MF, in addition to the following new observations: (*a*) we have identified significantly increased numbers of CCR10+ CD4+ cells is in MF patients' PBMCs without any other peripheral blood involvement as shown by routine laboratory tests, (*b*) CCR10 expression levels of individual circulating T cells do not vary according to MF disease stages, and (*c*) serum and skin CTACK/CCL27 are also elevated in patients with MF.

There is still the possibility that the CCR10 expression in our patients with MF is a reflection of inflammatory changes, as seen in atopic skin and in PBMCs of patients with severe drug reactions (11, 12). In fact, CCR10 is expressed by only 10% of CD4+ T cells in two models of inflammatory skin diseases (16), whereas it was expressed by 34% of MF lesion cells in our study. As shown in Fig. 3, there was no increase in CCR10 expression in atopic dermatitis cases. From these findings, we hypothesize that CCR10 is an important receptor involved in the pathophysiology of MF skin-homing and epidermotropism processes. In addition, the increase of CCR10+ CD4+ cells in the PBMCs of patients with MF is likely further proof that malignant, clonal T cells may already be circulating from early MF disease stages.

During skin-homing of peripheral T cells, chemokine interactions between CCR4, the thymus, and the activation-regulated

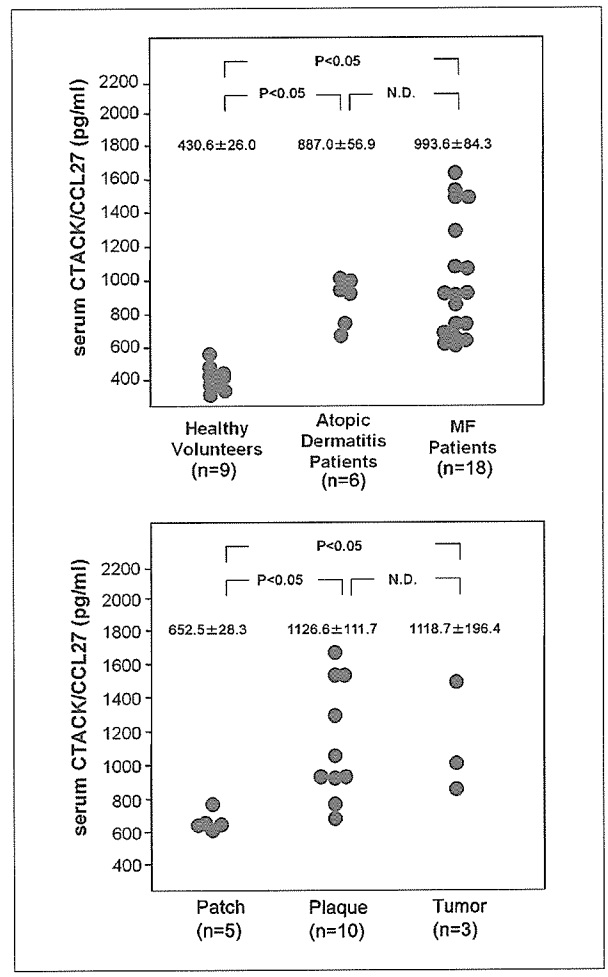

Fig. 5. Serum CTACK/CCL27 concentration assessed by ELISA. *Top,* both MF and atopic dermatitis patients have higher levels of CTACK/CCL27 than healthy volunteers. *Bottom,* a statistically significant elevation of serum CTACK/CCL27 levels was found between patch stage and other advanced stages.

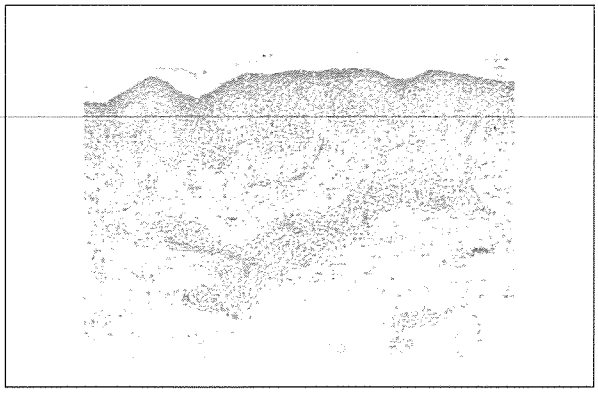

Fig. 6. Immunohistochemistry for CTACK/CCL27 in the MF skin tissue of patient 6 at the plaque stage. Generally, CTACK/CCL27 was expressed in suprabasal keratinocytes and endothelial cells of the superficial dermal plexus (original magnification, ×100).

chemokine (TARC/CCL17) have also been shown. Soler et al. reported that CCR10 is expressed only in a minor population of "effector-memory" skin-homing T cells, which respond to recently seen antigens (16). They also concluded that CCR10-CTACK interactions are not directly necessary for skin-homing, using anti-CTACK antibodies in the murine allergy model. Furthermore, CCR4 was expressed in other systemic cells than skin-homing T cells; hence, CCR10 might be more specific to the skin-homing population (11). Our study revealed that CCR10+ T cells were statistically elevated in patients with early MF than those from normal healthy controls or patients with atopic dermatitis, a common allergic skin reaction. Further studies are needed, but our study already suggests a role for CCR10-CTACK/CCR27 interactions during epidermotropism and skin-homing, not only in Sézary syndrome, but also in MF, by a subtly different pathway from other allergic skin reactions.

CTACK/CCL27, a functional ligand for CCR10, is predominantly expressed in basal keratinocytes of the epidermis (11). The concentration of CTACK/CCL27 around basal keratinocytes is rather high compared with other chemokines, playing a role in steady T cell trafficking into the skin (17). In our study, the serum CTACK/CCL27 concentration in patients with MF was significantly increased, which suggests a dynamic interaction between basal keratinocytes and malignant T cells.

Conversely, CCR4, another chemokine expressed by malignant T cells, also plays a central role in T helper 2–mediated cutaneous inflammation (18). A recent report revealed that TARC/CCL17, a ligand for CCR4, is significantly elevated in MF patients' serum, and that this is correlated with clinical and disease stages (19). It is also reported that TARC/CCL17 augments CTACK/CCL27 expression through tumor necrosis factor-α in atopic skin (20). These findings account for our observations that serum CTACK/CCL27 levels are elevated in patients with MF in accordance with the advance of the clinical stage. We believe that increases in the number of CCR10+ peripheral blood cells and serum CTACK/CCL27 levels may reflect the extent of increasing infiltration/inflammation during the course of the MF disease progress, as well as the importance of CCR4-TARC/CCL17 interactions during different disease stages.

A recent study has shown that single or multiple UV irradiation events can significantly down-regulate CTACK/CCL27 mRNA expression in mouse skin (21). Although no studies have been done to ascertain the relationship between CCR4 expression and UV therapy, one CTCL case has been reported in which the numbers of peripheral CCR4+ malignant T cells significantly decreased after retinoid plus psoralen UV A and IFN-γ therapy (22). These findings may explain one mechanism by which PUVA might be effective in treating CTCL skin lesions, by decreasing the affinity of skin-homing T cells and their rates of infiltration.

In summary, we have found that the CCR10+ CD4+ lymphocytes are significantly increased in the circulating PBMCs of patients with MF, regardless of clinical disease progression. An elevated concentration of serum CTACK/CCL27 was also noted in patients with MF, which together suggests an increase in lymphocyte skin-homing in the early stages of MF.

Acknowledgments

We thank Dr. James R. McMillan for critical proofreading of this manuscript.

References

1. Weinstock M, Horm J. Mycosis fungoides in the United States: increasing incidence and descriptive epidemiology. JAMA 1988;260:42–6.
2. Willemze R, Jaffe ES, Burg G, et al. WHO-EORTC classification for cutaneous lymphomas. Blood 2005;105:3768–85.
3. Washington LT, Huh YO, Powers LC, Duvic M, Jones D. A stable aberrant immunophenotype characterizes nearly all cases of cutaneous T-cell lymphoma in blood and can be used to monitor response to therapy. BMC Clin Pathol 2002;2:5.
4. Heald PW, Yan SL, Edelson RL, Tigelaar R, Picker LJ. Skin-selective lymphocyte homing mechanisms in the pathogenesis of leukemic cutaneous T-cell lymphoma. J invest Dermatol 1993;101:222–6.
5. Muche JM, Lukowsky A, Asadullah K, Gellrich S, Sterry W. Demonstration of frequent occurrence of clonal T cells in the peripheral blood of patients with primary cutaneous T-cell lymphoma. Blood 1997;90:1636–42.
6. Ferenczi K, Fuhlbrigge RC, Pinkus J, Pinkus GS, Kupper TS. Increased CCR4+ expression in cutaneous T cell lymphoma. J Invest Dermatol 2002;119:1405–10.
7. Campbell JJ, Haraldsen G, Pan J, et al. The chemokine receptor CCR4 in vascular recognition by cutaneous but not intestinal memory T cells. Nature 1999;400:776–80.
8. Sokolowska-Wojdylo M, Wenzel J, Gaffal E, et al. Circulating clonal CLA+ and CD4+ T cells in Sézary syndrome express the skin-homing chemokine receptors CCR4 and CCR10 as well as the lymph node-homing chemokine receptor CCR7. Br J Dermatol 2005;152:258–64.
9. Notohamiprodjo M, Segerer S, Huss R, et al. CCR10 is expressed in cutaneous T-cell lymphoma. Int J Cancer 2005;115:641–7.
10. Morales J, Homey B, Vicari AP, et al. CTACK, a skin-associated chemokine that preferentially attracts skin homing memory T cells. Proc Natl Acad Sci U S A 1996;96:14470–5.
11. Homey B, Alenius H, Muller A, et al. CCL27-10 interactions regulate T cell-mediated skin inflammation. Nat Med 2002;8:157–65.
12. Tapia B, Padial A, Sanchez-Sabate E, et al. Involvement of CCL27-10 interactions in drug-induced cutaneous reactions. J Allergy Clin Immunol 2004;114:335–40.
13. Reiss Y, Proudfoot AE, Power CA, Campbell JJ, Butcher EC. CC chemokine receptor (CCR) 4 and the CCR10 ligand cutaneous T cell-attracting chemokine (CTACK) in lymphocytic trafficking to inflamed skin. J Exp Med 2001;194:1541–7.
14. Kashani-Sabet M, McMillan A, Zackheim HS. A modified staging classification for cutaneous T-cell lymphoma. J Am Acad Dermatol 2001;45:700–6.
15. Hon KL, Leung TF, Ma KC, Li AM, Wong Y, Fok TF. Serum levels of cutaneous T-cell attracting chemokine (CTACK) as a laboratory marker of the severity of atopic dermatitis in children. Clin Exp Dermatol 2004;29:293–6.
16. Soler D, Humphreys TL, Spinola SM, Campbell

JJ. CCR4 versus CCR10 in human cutaneous Th lymphocytic trafficking. Blood 2003;101: 1677–83.
17. Bäumer W, Seegers U, Braun M, Tschernig T, Kietzmann M. TARC and RANTES, but not CTACK, are induced in two models of allergic contact dermatitis. Effects of cilomilast and diflorasone diacetate on T-cell-attracting chemokines. Br J Dermatol 2004; 151:823–30.
18. Vestergaard C, Bang K, Gesser B, Yoneyama H, Matsushima K, Larsen CG. A Th2 chemokine, TARC, produced by keratinocytes may recruit CLA+ CCR4+ lymphocytes into lesional atopic dermatitis skin. J Invest Dermatol 2000;115: 640–6.
19. Kakinuma T, Sugaya M, Nakamura K, et al. Thymus and activation-regulated chemokine (TARC/CCL17) in mycosis fungoides: serum TARC levels reflect the disease activity of mycosis fungoides. J Am Acad Dermatol 2003;48:23–30.
20. Vestergaard C, Johansen C, Christensen U, Just H, HohwyT, Deleuran M. TARC augmentsTNF-α-induced CTACK production in keratinocytes. Exp Dermatol 2004;13:551–7.
21. Rundhaug JE, Hawkins KA, Pavone A, et al. SAGE profiling of UV-induced mouse skin squamous cell carcinomas. comparison with acute UV irradiation effects. Mol Carcinog 2005;42:40–52.
22. Fujimura T, Aiba S, Yoshino Y, et al. CCR4 Expression by atypical T cells in systemic pilotropic lymphoma: its behavior under treatment with interferon γ, topical PUVA and systemic retinoid. Dermatology 2004;208: 221–6.

Graefe's Arch Clin Exp Ophthalmol
DOI 10.1007/s00417-005-0168-3

CLINICAL INVESTIGATION

Nobuyoshi Kitaichi
Tadamichi Shimizu
Ayumi Honda
Riichiro Abe
Kazuhiro Ohgami
Kenji Shiratori
Hiroshi Shimizu
Shigeaki Ohno

Increase in macrophage migration inhibitory factor levels in lacrimal fluid of patients with severe atopic dermatitis

Received: 28 April 2005
Revised: 17 September 2005
Accepted: 18 September 2005

N. Kitaichi (✉) · K. Ohgami · K. Shiratori · S. Ohno
Department of Ophthalmology and Visual Sciences, Hokkaido University Graduate School of Medicine, 060-8638, Sapporo, Japan
e-mail: nobukita@med.hokudai.ac.jp

T. Shimizu · A. Honda · R. Abe · H. Shimizu
Department of Dermatology, Hokkaido University Graduate School of Medicine, 060-8638, Sapporo, Japan

Abstract *Background and aims of the study:* Atopic dermatitis is a chronic inflammatory skin disorder that often involves some ophthalmic features. Macrophage migration inhibitory factor (MIF) is a proinflammatory cytokine that is associated with the generation of cell-mediated immune responses. Although serum MIF levels may be elevated in severe atopic dermatitis, the quantity of MIF in regional ocular fluid remains unknown. We measured MIF levels in tears (lacrimal fluid) of patients with atopic dermatitis. *Patients and methods:* Tear samples were collected from 16 patients with atopic dermatitis, 10 patients with allergic conjunctivitis, and 15 healthy control subjects. The clinical severity of atopic dermatitis was evaluated according to the Scoring Atopic Dermatitis (SCORAD) index. The index was calculated by summing the following scores: extent criteria, intensity criteria, and subjective symptoms. Macrophage migration inhibitory factor levels were determined by a human MIF enzyme-linked immunosorbent assay. All comparisons were two-tailed, and P values <0.01 were considered as statistically significant. *Results:* The mean MIF concentration in lacrimal fluid collected from healthy control subjects was 0.69± 0.2 ng/ml. The mean tear MIF levels were 17.87± 6.3 ng/ml in moderate-to-severe atopic dermatitis (SCORAD≥ 15, P=0.002), 0.93±0.08 ng/ml in mild atopic dermatitis (SCORAD< 15), and 2.76± 0.86 ng/ml in allergic conjunctivitis (P=0.008). *Conclusions:* A proinflammatory cytokine MIF level was elevated in tears as well as serum in cases of severe atopic dermatitis. These results suggest that MIF may play an important role in the induction or enhancement of ophthalmic features related to severe atopic dermatitis.

Keywords Allergic conjunctivitis · Atopic dermatitis · Eye · MIF · Serum · Tears

Introduction

Macrophage migration inhibitory factor (MIF) was first discovered in the late 1960s; it is therefore believed to be the first recognized lymphokine [6]. Since MIF was discovered as merely a part of the phenomenon of inhibiting migration of macrophages in the pre-molecular biology era, many scientists doubted its importance in the immune response. Investigations in the 1990s aimed at identifying novel systemic mediators that could regulate host inflammatory responses led to the identification of murine MIF as a product secreted by the anterior pituitary gland [2]. Upon stimulation, T cells release MIF, and MIF activity was first described as a product of cognate T-cell supernatants [15]. Macrophages have also been identified as an important source of MIF and are known to express MIF both constitutively and upon stimulation [15]. Macrophage migration inhibitory factor is considered to act by both paracrine and autocrine stimulatory pathways to augment the activation of these cells [15]. As reported

previously, MIF is essential for T-cell activation and possibly contributes to maintaining Th1/Th2 imbalance [1]. Increased MIF expression has been reported in lesions from many immune/inflammatory diseases, including psoriasis, glomerulonephritis, transplant rejection, neuro-Behçet's disease, asthma, adult respiratory distress syndrome, and inflammatory eye diseases [3, 4, 7, 11–13, 16, 17, 20, 22, 24].

Atopic dermatitis (AD) frequently involves some ophthalmic features: blepharitis, chronic keratoconjunctivitis, keratoconus, early-onset cataract, and rarely, retinal detachment [9]. AD is a chronic inflammatory skin disorder and many reports have documented its pathogenesis in relation to genetic and immunological abnormalities as well as environmental factors [10]. Although abnormal populations of Th1 and Th2 subsets of helper T cells (Th1/Th2 imbalance) have been identified as a cause of the pathogenesis of AD [8, 13, 25], a decrease in delayed-type hypersensitivity (DTH) is considered to involve more than Th1/Th2 imbalance in AD [5]. MIF is essential for T-cell activation and possibly contributes to maintaining Th1/Th2 imbalance as described above [1]. Also, a prominent increase in systemic MIF levels was detected in patients with severe AD, and the levels decreased when the clinical symptoms improved following treatment with corticosteroid ointment [18, 19]. We hypothesized that a high concentration of MIF could exist in the regional fluid of the eye as well as in serum in cases of severe atopic dermatitis. Because the Scoring Atopic Dermatitis (SCORAD) index, which is determined on the basis of several criteria related to lesion spread and intensity as well as on subjective signs, is commonly used to evaluate AD [21], AD patients were classified into two groups, as moderate-to-severe or mild AD, according to SCORAD index in the present study. We measured the MIF levels in tears (lacrimal fluid) of patients with AD and compared them to those of patients with allergic conjunctivitis (AC) and healthy people.

Materials and methods

Patients

We studied 16 patients with AD and 9 subjects with AC who visited the Departments of Dermatology and Ophthalmology, Hokkaido University Hospital, Sapporo, Japan. Atopic dermatitis is a common inflammatory disorder characterized by a chronic and relapsing course. In order to evaluate the severity of the disease as objectively as possible, the European Task Force on Atopic Dermatitis developed a method allowing consistent assessment by means of a severity index, called the Scoring Atopic Dermatitis (SCORAD) index [21]. The index should be calculated as a sum of the following scores: (1) extent criteria (involved surface area), (2) intensity criteria (erythema, edema/papulation, oozing/crusting, excoriation, and lichenification), and (3) subjective symptoms (pruritus and insomnia) [21]. We classified cases of AD in this study as "moderate-to-severe" (SCORAD≥15) or "mild" (SCORAD<15) according to the SCORAD index. Each patient with moderate-to-severe AD had atopic manifestations on the facial skin. Allergic conjunctivitis (AC) was diagnosed by slit lamp examination according to the guidelines of diagnosis and treatment of conjunctivitis, reported elsewhere [23]. Although we collected tear samples out of pollen season (December, January, and February), five of ten AC patients stated that they had sensitivity to grass or birch pollen. Most of the AC patients were considered to be in the chronic phase of AC, and their conjunctival signs and symptoms were mild. Tear samples were collected from 9 patients with severe AD (mean age, 26.1 years; age range, 18–37 years), 7 patients with mild AD (mean age, 29.0 years; age range, 16–44 years), 10 patients with AC (mean age, 32.6 years; age range, 22–44 years), and 15 healthy volunteers (mean age, 34.6 years; age range, 23–45 years). All subjects were Japanese, and healthy volunteers with no history of AD were recruited from our colleagues as controls. Dermatologists and ophthalmologists also verified no manifestations of AD and AC in controls when their tear/serum samples were collected. Informed consent was obtained from every patient and control subject.

Collection of tears and sera

All of the experiments in this study followed the tenets of the Declaration of Helsinki. After informed consent was obtained, tear samples were collected from all subjects. To obtain unstimulated basal lacrimal fluid, the tear samples (10 μl) were collected with microcapillary tubes for microhematocrit (75 mm length, Funakoshi, Tokyo) at the lateral canthus of patients in the supine position without any anesthesia. After obtaining informed consent, serum samples were collected from two of the severe AD patients whose tear MIF levels were quite high (>27.2 ng/ml), exceeding one standard deviation (SD) from the group's median value. Also, two subjects were chosen randomly from the patients with mild AD and healthy controls to measure their serum MIF levels.

Tear samples were centrifuged immediately at 4°C to remove cells and transferred into new tubes. Tear and serum samples were stored at −80°C until further examination.

Measurement of MIF

Macrophage migration inhibitory factor levels were determined by a human MIF enzyme-linked immunosorbent assay (ELISA) (CosmoBio, Tokyo, Japan) as described previously [18]. The kit contains all reagents necessary for performing the assay. Statistical analysis was performed using the Mann-Whitney U test.

Table 1 Values and significance of MIF levels in tears

	MIF levels (Mean MIF±SE)	*P* values vs. normal
Normal controls	0.69±0.2	-
AD: moderate to severe	17.87±6.3	0.002**
AD: mild	0.93±0.08	0.07
Allergic conjunctivitis	2.76±0.86	0.008**

AD Atopic dermatitis
**$P<0.01$ (Mann-Whitney U test, two-tailed)

Results

The mean MIF level in lacrimal fluid collected from healthy control subjects was 0.69±0.2 ng/ml. The mean tear MIF levels were 17.87±6.3 ng/ml in cases of moderate-to-severe AD (SCORAD≥15), 0.93±0.08 ng/ml in cases of mild AD (SCORAD<15), and 2.76±0.86 ng/ml in cases of allergic conjunctivitis (AC). Tear MIF levels were significantly elevated in patients with moderate-to-severe AD compared to normal controls ($P=0.002$, Table 1). The tear MIF levels of patients with AC were also higher than those of healthy subjects ($P=0.008$, Table 1). We did not, however, detect any significant difference in tear MIF levels between patients with mild AD (SCORAD<15) and healthy control subjects ($P=0.07$, Table 1).

We then focused on two cases of severe AD in which the tear MIF levels were higher than 27.2 ng/ml, i.e., more than one standard deviation (SD) from the group's median value. Both had the severest skin manifestations of atopic dermatitis in this study when their tears were collected. After informed consent was obtained from these patients, serum samples were drawn and the serum MIF levels were measured. As shown in Table 2, their serum MIF levels were approximately equivalent to those in the lacrimal fluid of patients with severe AD. In contrast, although the serum MIF levels in cases of mild AD were still elevated compared to those of healthy controls, their MIF concentrations in tears were no higher than those of healthy controls (Table 2).

Table 2 MIF concentrations of tears and sera

Cases	Age/sex	Tear MIF (ng/ml)	Serum MIF (ng/ml)
1. AD: severe	20/M	63.4	79.7
2. AD: severe	35/M	30.1	42.0
3. AD: mild	44/F	0.9	17.5
4. AD: mild	16/M	0.7	12.2
5. Control	45/F	0.8	4.7
6. Control	24/F	1.0	3.2

AD Atopic dermatitis

Discussion

In the present study, we detected high levels of MIF in the lacrimal fluid of patients with severe AD. We previously reported an increase in serum MIF levels in patients with AD [18]. Although AD frequently involves some ophthalmic features (blepharitis, chronic keratoconjunctivitis, keratoconus, early-onset cataract, and retinal detachment), how MIF behaves in the ocular fluid of patients with AD remained unknown. We wished to determine how tear MIF levels of patients with severe AD compared with AC and healthy subjects.

MIF is expressed and secreted in many tissues: in the brain, eye (lens, corneal epithelial cells, iris, ciliary body, and retina), ear, immune cells (thymus, spleen, lymph nodes, blood, and bone marrow, by monocytes, macrophages, T cells, B cells, dendritic cells, eosinophils, basophils, neutrophils, and mast cells), lungs, breast, endocrine systems (pituitary gland, adrenal cortex, and pacreas), liver, testis, prostate, ovaries, gastrointestinal tract, kidney, fat tissue, skin (by keratinocytes, sebaceous glands, hair follicles, endothelial cells and fibroblasts), bone, and joints [4]. This study demonstrated that tear MIF concentration is significantly higher in patients with severe AD than in controls. Patients with AC also showed significantly higher levels of MIF than healthy controls; however, there were vast differences between the averages of AD and AC groups.

Since MIF levels in tears were elevated for both diseases involving the immune system, one possible source of tear MIF is the lymphocytes in conjunctival follicles. Another possible cause of the elevation of tear MIF levels in the eyes may be the lacrimal gland, but no study has been performed to determine if the lacrimal gland expresses or secretes MIF or not. A third possible source may be peripheral blood mononuclear cells (PBMCs) [14]. As previously reported, a substantial increase in systemic MIF levels was detected in patients with severe AD, and the levels decreased when the skin symptoms improved following treatment with corticosteroid ointment [18]. Furthermore, the elevated serum MIF was due to secretion from systemic PBMC [18, 19]. We found two patients with severe AD who showed extremely high levels (in excess of 30 ng/ml) of MIF in this study. To examine how blood PBMC contributes to MIF levels in lacrimal fluid, we collected serum samples from AD patients as well as tears. Because a very high serum MIF concentration was detected in both of these patients (Table 2) and the space of the oculi is limited, some proportion of MIF in tears may be attributable to a systemic increase in MIF. The secretion of MIF from PBMCs might contribute to the elevation of tear MIF levels more than regional inflammatory cells of the eyes in patients with severe AD. Since we did not collect blood samples from AC subjects, it is still unclear how much blood PBMC contributes to tear MIF levels in cases of AC. In the present study, AC patients did not have

obvious systemic inflammation, but local. Moreover, we detected higher tear MIF levels in the AC group than in the mild AD group, suggesting that MIF may be secreted in the eye to some extent. Further studies might be required in vernal or other etiologies of conjunctivitis, as well as for treated vs. untreated AC to clarify eye-derived MIF in tears.

This is the first report that MIF concentrations in tears are elevated in cases of severe AD in humans. In conclusion, MIF in regional ocular fluid may be involved in the induction or enhancement of ophthalmic features caused by severe AD.

Acknowledgements The authors are grateful to Dr. Hiroshi Fujishima and Dr. Kazumi Fukagawa (Department of Ophthalmology, Tokyo Dental College, Ichikawa, Japan) for their technical cooperation. This study was supported by a Grant-in-Aid for Research from the Ministry of Education, Culture, Sports, Science, and Technology (MEXT) Japan, a Grant for Research on Sensory and Communicative Disorders from The Ministry of Health, Labor, and Welfare, Japan, and by Research Fellowships of Japan Society for the Promotion of Science (JSPS) for Young Scientists.

References

1. Bacher M, Metz CN, Calandra T, Mayer K, Chesney J, Lohoff M, Gemsa D, Donnelly T, Bucala R (1996) An essential regulatory role for macrophage migration inhibitory factor in T-cell activation. Proc Natl Acad Sci USA 93 (15):7849–7854
2. Bernhagen J, Calandra T, Mitchell RA, Martin SB, Tracey KJ, Voelter W, Manogue KR, Cerami A, Bucala R (1993) MIF is a pituitary-derived cytokine that potentiates lethal endotoxaemia. Nature 365 (6448):756–759
3. Brown FG, Nikolic-Paterson DJ, Chadban SJ, Dowling J, Jose M, Metz CN, Bucala R, Atkins RC (2001) Urine macrophage migration inhibitory factor concentrations as a diagnostic tool in human renal allograft rejection. Transplantation 71 (12):1777–1783
4. Calandra T, Roger T (2003) Macrophage migration inhibitory factor: a regulator of innate immunity. Nat Rev Immunol 3 (10):791–800
5. Cooper KD (1994) Atopic dermatitis: recent trends in pathogenesis and therapy. J Invest Dermatol 102 (1):128–137
6. David JR (1966) Delayed hypersensitivity in vitro: its mediation by cell-free substances formed by lymphoid cell-antigen interaction. Proc Natl Acad Sci USA 56 (1):72–77
7. Donnelly SC, Haslett C, Reid PT, Grant IS, Wallace WA, Metz CN, Bruce LJ, Bucala R (1997) Regulatory role for macrophage migration inhibitory factor in acute respiratory distress syndrome. Nat Med 3 (3):320–323
8. Holden CA (1993) Atopic dermatitis-messengers, second messengers and cytokines. Clin Exp Dermatol 18 (3):201–207
9. Kanski JJ (2003) Clinical Ophthalmology, a systematic approach, 5th edn. Buttherworth-Heinemann/ Elsevier Science, Edinburgh, UK
10. Kapp A (1995) Atopic dermatitis-the skin manifestation of atopy. Clin Exp Allergy 25 (3):210–219
11. Kitaichi N, Kotake S, Mizue Y, Matsuda H, Onoé K, Nishihira J (2000) Increase of macrophage migration inhibitory factor in sera of patients with iridocyclitis. Br J Ophthalmol 84 (12):1423–1425
12. Kitaichi N, Kotake S, Sasamoto Y, Namba K, Matsuda A, Ogasawara K, Onoé K, Matsuda H, Nishihira J (1999) Prominent increase of macrophage migration inhibitory factor in the sera of patients with uveitis. Invest Ophthalmol Vis Sci 40 (1):247–250
13. Lan HY, Yang N, Nikolic-Paterson DJ, Yu XQ, Mu W, Isbel NM, Metz CN, Bucala R, Atkins RC (2000) Expression of macrophage migration inhibitory factor in human glomerulonephritis. Kidney Int 57 (2):499–509
14. Lever R, Turbitt M, Sanderson A, MacKie R (1987) Immunophenotyping of the cutaneous infiltrate and of the mononuclear cells in the peripheral blood in patients with atopic dermatitis. J Invest Dermatol 89 (1):4–7
15. Morand EF, Bucala R, Leech M (2003) Macrophage migration inhibitory factor: an emerging therapeutic target in rheumatoid arthritis. Arthritis Rheum 48 (2):291–299
16. Niino M, Ogata A, Kikuchi S, Tashiro K, Nishihira J (2000) Macrophage migration inhibitory factor in the cerebrospinal fluid of patients with conventional and optic-spinal forms of multiple sclerosis and neuro-Behcet's disease. J Neurol Sci 179 (S 1–2):127–131
17. Rossi AG, Haslett C, Hirani N, Greening AP, Rahman I, Metz CN, Bucala R, Donnelly SC (1998) Human circulating eosinophils secrete macrophage migration inhibitory factor (MIF). Potential role in asthma. J Clin Invest 101 (12):2869–2874
18. Shimizu T, Abe R, Ohkawara A, Mizue Y, Nishihira J (1997). Macrophage migration inhibitory factor is an essential immunoregulatory cytokine in atopic dermatitis. Biochem Biophys Res Commun 240 (1):173–178
19. Shimizu T, Abe R, Ohkawara A, Nishihira J (1999) Increased production of macrophage migration inhibitory factor by PBMCs of atopic dermatitis. J Allergy Clin Immunol 104 (3 Pt 1): 659–664
20. Shimizu T, Nishihira J, Mizue Y, Nakamura H, Abe R, Watanabe H, Ohkawara A, Shimizu H (2001) High macrophage migration inhibitory factor (MIF) serum levels associated with extended psoriasis. J Invest Dermatol 116 (6):989–990
21. Stadler J (1993) Severity scoring of atopic dermatitis: the SCORAD index. Consensus report of the European Task Force on Atopic Dermatitis. Dermatology 186 (1):23–31
22. Sustiel A, Rocklin R (1989) T cell responses in allergic rhinitis, asthma and atopic dermatitis. Clin Exp Allergy 19 (1):11–18
23. Uchio E, Ono SY, Ikezawa Z, Ohno S (2000) Tear levels of interferon-gamma, interleukin (IL) -2, IL-4 and IL-5 in patients with vernal keratoconjunctivitis, atopic keratoconjunctivitis and allergic conjunctivitis. Clin Exp Allergy 30 (1):103–109
24. Yamaguchi E, Nishihira J, Shimizu T, Takahashi T, Kitashiro N, Hizawa N, Kamishima K, Kawakami Y (2000) Macrophage migration inhibitory factor (MIF) in bronchial asthma. Clin Exp Allergy 30 (9):1244–1249
25. Zachary CB, Allen MH, MacDonald DM (1985) In situ quantification of T-lymphocyte subsets and Langerhans cells in the inflammatory infiltrate of atopic eczema. Br J Dermatol 112 (2):149–156

research articles Journal of proteome research

Proteomic and Bioinformatic Characterization of the Biogenesis and Function of Melanosomes

An Chi,[†,#] Julio C. Valencia,[‡,#] Zhang-Zhi Hu,[§,#] Hidenori Watabe,[‡] Hiroshi Yamaguchi,[‡] Nancy J. Mangini,[∥] Hongzhan Huang,[§] Victor A. Canfield,[⊥] Keith C. Cheng,[○] Feng Yang,[†] Riichiro Abe,[▽] Shoichi Yamagishi,[+] Jeffrey Shabanowitz,[†] Vincent J. Hearing,[‡] Cathy Wu,[§] Ettore Appella,[*,‡] and Donald F. Hunt[*,†,¶]

Department of Chemistry, University of Virginia, Charlottesville, Virginia, 22904, Laboratory of Cell Biology, National Institutes of Health, Bethesda, Maryland, 20892, Protein Information Resource, Georgetown University Medical Center, Washington, DC, Indiana University School of Medicine—Northwest, Gary, Indiana, Department of Pharmacology, Pennsylvania State University College of Medicine, Hershey, Pennsylvania, Jake Gittlen Cancer Research Foundation, Pennsylvania State University College of Medicine, Hershey, Pennsylvania, Department of Dermatology, Hokkaido University Graduate School, Sapporo, Japan, Kurume University School of Medicine, Kurume, Japan, and Department of Pathology, University of Virginia, Charlottesville, Virginia, 22908

Received July 21, 2006

Melanin, which is responsible for virtually all visible skin, hair, and eye pigmentation in humans, is synthesized, deposited, and distributed in subcellular organelles termed melanosomes. A comprehensive determination of the protein composition of this organelle has been obstructed by the melanin present. Here, we report a novel method of removing melanin that includes in-solution digestion and immobilized metal affinity chromatography (IMAC). Together with in-gel digestion, this method has allowed us to characterize melanosome proteomes at various developmental stages by tandem mass spectrometry. Comparative profiling and functional characterization of the melanosome proteomes identified ~1500 proteins in melanosomes of all stages, with ~600 in any given stage. These proteins include 16 homologous to mouse coat color genes and many associated with human pigmentary diseases. Approximately 100 proteins shared by melanosomes from pigmented and nonpigmented melanocytes define the essential melanosome proteome. Proteins validated by confirming their intracellular localization include PEDF (pigment-epithelium derived factor) and SLC24A5 (sodium/potassium/calcium exchanger 5, NCKX5). The sharing of proteins between melanosomes and other lysosome-related organelles suggests a common evolutionary origin. This work represents a model for the study of the biogenesis of lysosome-related organelles.

Keywords: proteomics • organelles • lysosome related • biogenesis

Introduction

Melanosomes are membrane-bound organelles, specialized in the production and distribution of melanin pigment, that are conserved in structure from primitive organisms to mammals. In lower species, melanin pigmentation plays important roles in thermoregulation, camouflage, and sexual attraction. In humans, melanin in the skin, hair, and eyes protects the body against environmental challenges such as solar UV exposure, toxic free radicals, and heavy metals. Variations in chemical composition, melanosome structure, and distribution result in distinct skin, hair, and eye color differences in human populations. Dysfunctions in pigmentation and melanosome biogenesis are associated with a wide variety of inherited genetic disorders and pigmentary diseases, including oculocutaneous albinism and Hermansky–Pudlak syndrome. Melanosome-specific proteins also provide important markers for malignant melanoma.

To date, about 125 genes affecting mammalian pigmentation have been identified,[1] about half of which have been cloned. Six of these genes encode proteins that are specifically localized in melanosomes including enzymatic and structural compo-

* Authors for correspondence. For Dr. Ettore Appella: Building 37, Room 2140, National Institutes of Health, Bethesda, MD 20892; e-mail, appellae@nih.gov. For Dr. Donald F. Hunt: Department of Chemistry, University of Virginia, McCormick Road, P.O. Box 400319, Charlottesville, VA 22904, E-mail: dfh@virginia.edu.

† Department of Chemistry, University of Virginia.

# These authors contributed equally to this research.

‡ Laboratory of Cell Biology, National Institutes of Health.

§ Department of Biochemistry and Molecular & Cellular Biology, Georgetown University Medical Center.

∥ Indiana University School of MedicinesNorthwest.

⊥ Department of Pharmacology, Pennsylvania State University College of Medicine.

○ Jake Gittlen Cancer Research Foundation, Pennsylvania State University College of Medicine.

▽ Hokkaido University Graduate School.

+ Kurume University School of Medicine.

¶ Department of Pathology, University of Virginia.

10.1021/pr060363j CCC: $33.50

Published on Web 10/04/2006

nents required for melanin biosynthesis.[2] The specific roles of more than 80 proteins previously identified in melanosomes[3] have yet to be defined. In mammals, melanosomes mature from undifferentiated vesicles (stage I) to elongate and form internal fibrils (stage II).[2,4,5] In the presence of tyrosinase and other enzymes, melanin is synthesized and deposited on the internal fibrils (stage III) and can become uniformly dense (stage IV) in heavily pigmented melanocytes. As melanosomes mature, they are gradually transported to the peripheries of the melanocytes in which they form and, in human skin, are transferred to neighboring keratinocytes.

A detailed understanding of how melanosomes mature and move within and between cells requires a comprehensive knowledge of proteins comprising them. Although methods for isolating melanosomes at various developmental stages have been established,[2,3,6] obtaining them in sufficient quantities and removing endogenous melanins remains challenging. Melanins are highly heterogeneous polymers of various quinones, indoles, indole-quinones, and sulfhydryl derivatives[7,8] that can covalently bind to proteins, causing difficulties in solubilization. Even small amounts of melanin result in motility shifts that adversely affect electrophoretic resolution of proteins, block antibody epitopes needed for Western blotting, and bind to chromatographic columns, degrading liquid chromatography/mass spectrometry (LC/MS) performance. Pursuit of a proteomic analysis of melanosomes, thus, required an effective approach for purifying and solubilizing them, and removing the melanin.

Global melanosome proteome characterization was made possible by using LC/MS to analyze both in-solution digests after removal of melanin by immobilized metal affinity chromatography (IMAC)[9] and in-gel digests. Proteins identified in various maturation stages by LC/MS were organized into families or subgroups based on functional classifications such as gene ontology (GO).[10] A combination of immunoblotting, immunofluorescence microscopy, and bioinformatics analysis was used to characterize the protein profiles of melanosomes at various developmental stages. The stage-related proteins provide direct evidence of protein sorting and trafficking to this organelle and information about their biogenesis as lysosome-related organelles. Further, 17 of the 63 human homologues of mouse pigment gene products were identified in various melanosome stages.

Materials and Methods

Cell Cultures and Biochemical Procedures. Pigmented (MNT-1) and nonpigmented (SK-MEL-28) human melanoma cells were cultured, and various stages of melanosomes were isolated by sucrose density gradients, as described previously.[2,3,6]

In-Gel Trypsin Digestion. Early stage melanosomes (150 μg) were solubilized directly in sample loading buffer and were separated on 10% SDS-PAGE gels, according to the manufacturer's instructions (Bio-Rad Laboratories, Inc., Hercules, CA). Gels were stained with colloidal Coomassie blue for 1 h and were then destained in water (Bio-Rad). Lanes containing samples were cut into 15 slices from the top to the bottom of the gel. In-gel trypsin (Promega Corp., Madison, WI) digestion was performed as previously described.[11] Peptides from bands of similar staining intensity were pooled together, while peptides from dark bands were analyzed individually.

In-Solution Digestion. Late stage protein pellets (150 μg) were frozen and thawed three times before being solubilized in a mixture of 8 M urea and 10% acetonitrile in 100 mM ammonium bicarbonate (Sigma-Aldrich, St. Louis, MO). Each sample was sonicated briefly and mixed using a vortexer. Samples were then reduced with 10 mM dithiothreitol (Sigma-Aldrich) at 51 °C for 1 h and carboxyamidomethylated with 20 mM iodoacetamide (Sigma-Aldrich) in the dark at room temperature for 45 min. Endo-Protease Lys-C (Roche Diagnostics, Indianapolis, IN) was then added to each sample (1:20 enzyme/protein ratio) after diluting the urea to 4 M with 100 mM ammonium bicarbonate (pH 8.5). After digestion for 6 h at room temperature, samples were further diluted with 100 mM ammonium bicarbonate until the final urea concentration reached 1 M. Trypsin (1:20 enzyme/protein ratio) was added at room temperature for 10 h at pH 8.5.

IMAC Melanin Removal. IMAC columns were constructed as previously described[12] with some modifications. Briefly, a 360 μm o.d. × 200 μm i.d. (Polymicro Technologies, Inc., Phoenix, AZ) fused-silica column was packed with 8 cm Poros 20MC resin (PerSeptive Biosystem, Framingham, MA). The IMAC column was washed for 5 min with 50 mM EDTA (Sigma-Aldrich), pH 9, followed by a 5 min wash with NANOPure (Barnstead, Dubuque, IA) water to bring the pH back to neutral. The columns were then activated with 100 mM $FeCl_3$ (Sigma-Aldrich) at a flow rate of 2 μL/min for 10 min. Excess $FeCl_3$ was removed with 5−10 column volumes of 0.01% acetic acid (Sigma-Aldrich). A fused-silica precolumn (360 μm o.d. × 75 μm i.d.) packed with irregular C18 beads (5 μm, ODS-AQ, YMC, Waters, Milford, MA) was then end-connected to the IMAC column using a Teflon sleeve (0.012 in. o.d. × 0.060 in. i.d., Zeus, Orangerburg, SC). An aliquot of the in-solution digest sample was directly loaded onto the IMAC/C18 reverse-phase precolumn assembly. The precolumn alone was then washed with 0.1% acetic acid to remove contaminating salts.

In-Gel Tryptic Digest Analyzed with 3D Ion Trap Mass Spectrometer. An aliquot of the in-gel tryptic digest was loaded onto a C18 reverse-phase precolumn (360 μm o.d. × 75 μm i.d.). For sample analysis by mass spectrometry, the precolumn was Teflon-sleeve-connected to an analytical reverse-phase HPLC column (360 μm o.d. × 50 μm i.d.) packed with 5 cm regular C8 beads (5 μm, ODS-AQ, YMC). Each sample was then analyzed by on-line nanoflow RP-HPLC (Agilent 1100, Palo Alto, CA) interfaced to a microelectrospray ionization source of a LCQ^{DecaXP} mass spectrometer (Thermo Electron, San Jose, CA) that was operated in the data-dependent MS/MS mode on the 5 most abundant ions detected in precursor MS scans, as previously described.[13] The HPLC gradient (buffer A = 100 mM acetic acid in water, buffer B = 70% acetonitrile/100 mM acetic acid in water) was 0−5% B in 5 min, 5−40% B in 180 min, 40−60% B in 30 min, 60−100% B in 10 min, 100% B in 2 min, and 100−0% B in 5 min. Full scan mass spectra were acquired over an m/z = 300−2000 range.

In-Solution Tryptic Digest Analyzed with Hybrid Linear Ion Trap-Fourier Transform Mass Spectrometer. The precolumn loaded with the melanin-depleted sample was Teflon-sleeve-connected to an analytical reverse-phase HPLC column (360 μm o.d. × 50 μm i.d.) with an integrated electrospray emitter tip as previously described.[13] Samples were analyzed by nanoflow RP-HPLC micro-ESI coupled to an LTQ-FT hybrid linear ion trap-Fourier transform mass spectrometer (Thermo Electron). The instrument was cycled through a single (FT) MS experiment followed by 10 data-dependent (LTQ) MS/MS experiments. Gas-phase fractionation in the mass-to-charge (m/z) dimension[14] was employed such that the following

segmented m/z ranges were selected in series for MS precursor ion selection: m/z 300−500, 500−700, 700−900, 900−1200, and 1200−2000. For m/z 500−700 and 700−900, the HPLC gradient used was 0−5% B in 5 min, 5−40% B in 180 min, 40−60% B in 30 min, 60−100% B in 10 min, 100% B in 2 min, and 100−0% B in 5 min; for the other m/z ranges, a shorter HPLC gradient (0−5% B in 5 min, 5−60% B in 60 min, 60−100% B in 10 min, 100% B in 2 min, and 100−0% B in 5 min) was used.

Data Analysis. Acquired data were searched against the human database [National Center for Biotechnology Information (NCBI)] with SEQUEST.[9] All SEQUEST search parameters were conducted with "no enzyme" specificity and a static modification of 57 Da on cysteine, representing alkylation with iodoacetamide, and a differential modification of 16 Da on methionine, representing the possibility of oxidation. For data acquired from in-gel digests on the LCQ^{DecaXP}, the precursor mass window was set to ±3 Da (amu), and fragment ion mass tolerance was set to 0.35 Da (amu). For data acquired from in-solution digests on the LTQ-FT, the precursor mass window was set to ±0.05 Da (amu), and the fragment ion mass tolerance was set to 0.35 Da (amu). SEQUEST search results were evaluated by the following parameters prior to manual validation: DelMass < 1.0, Xcorr > 2.4, DelCn > 0.1, Sp > 500, RSp < 10, Ion Ratio > 0.6.

Bioinformatics Analysis. Systematic bioinformatics analysis of the melanosome proteomes was conducted using the PIR *i*ProXpress system,[15] which provides functionalities for peptide and protein mapping and functional annotation and profiling. Protein lists and peptide sequences generated from proteomic experiments were mapped to UniProt Knowledgebase (UniProtKB)[16] entries based on ID and peptide mappings. The ID mapping, through the UniProt/PIR ID mapping service,[16] maps protein/gene IDs from about 30 data sources (including NCBI identifiers such as gi number, Entrez Gene and RefSeq ID) to UniProtKB. For many-to-one mapping, where multiple IDs map to the same UniProtKB protein, as is often the case for gi numbers, the mapping effectively removes redundancy. For proteins not mapped through ID mapping, their peptide sequences are searched against the UniProtKB for sequence mapping to assign the protein ID. In the case of one-to-many mapping, if all the matched entries are in the same UniRef90 cluster, in which members share at least 90% sequence identity, one representative sequence is chosen. If the proteins belong to different UniRef90 clusters, assignment is made with retroinspection and manual validation of the original MS/MS protein identification results. When both ID and peptide mappings were combined, a total of 1438 UniProtKB entries were mapped from proteomic data in this study. Following the protein mapping, a protein information matrix was generated to describe all melanosome proteins based on sequence analysis and extensive annotations extracted from the *i*ProClass[14] database. *i*ProClass integrates annotations from over 90 biological databases for all UniProtKB proteins, including protein name, family classification, isoform, sequence features (domain, motif, and functional site), GO (molecular function, biological process, and cellular component), function and functional category, structure and fold classification, pathway and pathway category, protein−protein interaction and complex, and post-translational modification. The profiling analysis involved functional categorization of proteins and cross-comparison of coexpressed or differentially expressed proteins from multiple datasets to discover plausible functions and pathways. The melanosome proteome datasets in this study were organized into 12 subsets according to stage and cell type (Supplementary Table 1, Supporting Information). Iterative categorization and sorting of protein attributes, especially of GO classes and pathways (KEGG and BioCarta), revealed major functional categories in the proteome. Interesting unique or common proteins at different stages of melanosome biogenesis were identified by manual examination and comparison of these functional profiles from the melanosome data subsets. Organelle proteomes reported for lysosomes, endoplasmic reticulum, synaptosomes, neuromelanin granules, exosomes, and platelet were also incorporated into the matrix for comparison with the melanosome proteome.

Immunochemical Techniques. For dual immunofluorescence, cells were seeded in 2-well chamber slides (Nalgene, Naperville, IL), fixed, and stained as described previously.[17] SLC24A5 polyclonal antibodies were generated in rabbits and chickens against synthetic peptides corresponding to sequences at the carboxy terminal region of human SLC24A5 and were affinity-purified prior to use. Other antibodies used are noted in the legend to Figure 2 and were obtained from sources as cited in the text. Images were obtained using an LSM 510 confocal microscope (Zeiss, Jena, Germany). Analysis and quantification of the colocalization signal was evaluated under equal microscope parameters using Zeiss colocalization software. For Western blotting, extracts of cells and of melanosomes were separated by SDS-PAGE and were subjected to Western blotting as reported previously.[17]

Results

Comparative Profiling of Melanosome Proteomes. Characterizing the melanosomal proteome is especially challenging due to the inefficient solubilization of highly hydrophobic membrane proteins[18−20] and contamination with endogenous melanin. After screening a number of solvent conditions to solubilize melanosomes, we found that a combination of urea and 10% acetonitrile was highly effective. Black melanosome pellets were gradually solubilized on a shaker for ~10 h, and the sample became light brown after 12 h of subsequent digestion with trypsin. We then took advantage of the heavy metal ion[21,22] sequestering property of melanin by loading the resulting peptides onto an IMAC column activated with an excess volume of $FeCl_3$, assembled back-to-back with an RP precolumn. The melanin was retained on the IMAC column due to the high affinity of Fe(III) for the *o*-diOH groups of melanin,[23] while the peptides passed through and were subsequently caught on the C18 reverse-phase precolumn. This assembly allows the efficient and concurrent removal of melanin and the loading of the sample onto the column in a single step prior to the LC/MS analysis.

Proteomic analysis was applied to stages I and II melanosomes purified from pigmented (MNT1) or from unpigmented (SK-MEL-28) human melanoma cells, and to stage IV melanosomes from MNT1 cells. About 600 (range 551−652) distinct proteins were detected in each preparation. Proteins identified were grouped into 12 subsets according to stage and cell type (Supplementary Table 1, Supporting Information). Proteins unique to unpigmented SK-MEL-28 melanosomes "Unique SK-MEL-28" or to pigmented MNT1 melanosomes "Unique MNT1" are likely involved in the regulation of pigmentation, whereas proteins in the MNT1 stage IV ("Unique late stage") group may be related to melanosome maturation.

About 100 proteins were common among all stages of melanosomes isolated from MNT1 and from SK-MEL-28 cells ("Common all stages") (Supplementary Table 2, Supporting Information). Unlike-stage-related or cell type-specific melanosome proteins, these common proteins are considered constituent proteins or resident proteins of melanosomes. Interestingly, these proteins are associated with several other cellular compartments that collectively may represent the basic components necessary to define melanosomes. About 25% of these proteins are potential transmembrane proteins with various functions, including ion/solute transporters, receptors, and membrane trafficking proteins. Over 33% are enzymes with heterogeneous and broad catalytic activities (oxidoreductases, transferases, hydrolases, lyases, and isomerases). Other proteins include molecular motor and cytoskeleton proteins, and potential signaling molecules. There are also proteins known to be associated with the plasma membrane (e.g., Na,K-ATPase subunits) and other organelles, such as the endoplasmic reticulum (e.g., ribophorin I, GRP 78/BiP, and calnexin) and lysosomes (e.g., cathepsin D, B, and γ-Glu-X carboxypeptidase). The presence of vacuolar proton ATPases (e.g., vATPases A, B, H, and the clathrin coated vesicle/synaptic vesicle proton pump) in both early and late melanosomes is consistent with the critical importance of pH in regulating the physiological functions of melanosomes.[24,25] In addition, the presence of sulfhydryl enzymes (e.g., glutathione *S*-transferase pi, protein disulfide isomerases, and quinone reductase) indicates their likely importance in regulating melanin synthesis, since pheomelanins, a major subclass of melanins, contain sulfur.

Proteins participating in membrane dynamics also represent a major component of the melanosome proteome.The identification of regulatory molecules involved in cellular protein sorting and trafficking, vesicle formation, docking, and fusion emphasizes the critical nature of melanosome interactions with other subcellular components. These include trafficking proteins (e.g., SEC22b), synaptic vesicle-associated proteins (e.g., VAT-1), lipid raft-associated proteins (e.g., stomatin and flotillin-1), secretory vesicle-associated proteins (e.g., calumenin), and Ca^{2+}-dependent annexin proteins (organizers of membrane domains and membrane-recruitment platforms). In addition, elements of the cytosolic fusion machinery important for organelle biogenesis, for example, SNARE proteins and small GTPase family members and related proteins (RABs) (e.g., Rab7, Rab27a, Rab5c, and P21-rac1), were also identified. As shown in Supplementary Table 3 (Supporting Information), a total of 18 RABs was identified in early melanosomes from MNT1 and SK-MEL-28 cells, some of which were detected only in stage I or only in stage II melanosomes.

Of special note are proteins known to be present both in endocytic and in secretory pathways. For example, Pmel17, one of the six known melanosomal-specific proteins, reaches the cell surface and is internalized by receptor-mediated endocytosis;[26,27] it has been widely studied as an immunotherapy target for melanoma.[28]

Identification and Validation of Stage-Related Melanosomal Proteins. Proteins present in individual stages of melanosomes can potentially play important roles in melanosome morphogenesis. Table 1 shows a list of putative stage-related proteins of special interest from the MNT1 melanosome proteome. There are over twice as many unique proteins in stage IV than there are in early stages of the melanosome, which may reflect the complex functions of mature melanosomes. We selected several interesting targets for validation by immunoblotting and immunofluorescence analysis, including proteins more abundant in some stages and those distributed similarly among the stages (Figure 1).

Pigment-epithelium derived factor (PEDF) is a potent inhibitor of angiogenesis and is a potent inductor of Fas-ligand-dependent apoptosis.[29] Dual immunofluorescence revealed that PEDF has a granular distribution in the cytoplasm of MNT-1 cells and does not colocalize with the stage II melanosome marker HMB-45 (Figure 1B) or the lysosomal marker LAMP1 (not shown). The pattern is similar to that of Pmel17 stained by αPEP13h (a stage I melanosome marker). Two PEDF bands were recognized by immunoblotting: a major band at 50 kDa, which corresponds to full-length PEDF (418 aa) and is most abundant in stage I melanosomes; and a minor band at 37 kDa (possibly a truncated form), which was distributed throughout the melanosome fractions.

We validated the presence of integrin $\beta 1$ (I$\beta 1$), a cell surface protein involved in melanoma cell migration[30] that sorts through the secretory pathway.[31] I$\beta 1$ was highly enriched in stage I melanosomes (as well as late melanosomes) and showed partial colocalization with Pmel17 in granular structures near the perinuclear area. Since the early endosome marker (EEA1) is present in stage I melanosomes, we next validated the presence of Rab5, which directs the fusion of early endosomes, is recruited to endocytic vesicles, and is present in sorting endosomes.[32] Rab5 was highly enriched in stage I melanosomes, but was also detected in other stages. Dual immunofluorescence shows limited colocalization of Rab5 and Pmel17 in granular structures. These results are consistent with reports that early endosome markers can be found, in lesser amounts, in stage II melanosomes.[33]

In late-stage melanosomes, we confirmed the presence of the G2 subunit of vATPase which supports the important role of this pump in regulating pH, melanin production, and organelle stabilization. SLC24A5, a cation exchanger that transports Ca^{2+} and K^+ in exchange for Na^+, is also present in greater abundance in late melanosomes. As recently reported, SLC24A5 is involved specifically in melanogenesis and in the formation of pigmented granules.[34]

Melanosome Proteins Mapped to Known Mouse Coat Color Genes. Currently, 63 cloned mouse coat color genes have human homologues, and many are associated with inherited human pigmentary diseases [http://ifpcs.med.umn.edu/micemut.htm]. Among these human homologues, 16 proteins were identified in this proteomics analysis (Table 2), including 6 previously validated melanosome proteins and 10 new ones. Four of those had been identified and validated as specific melanosomal proteins (Tyr, Tyrp1, si/Pmel17, and OA1).[3,5,35,36] Two others (Rab27a and Rab38) had also been identified as melanosomal proteins,[37,38] although not specific to those organelles. In this study, we identified 10 novel proteins that map to coat color genes as melanosomal components. Although further analyses will be required to confirm their specificity for melanosomes and their possible functions there, several have known activities plausibly related to melanosome function. For example, Atp7a is a copper transport protein, and copper is a critical metal ligand required for tyrosinase function.[39] Golden has recently been shown to be important to determining constitutive levels of human skin pigmentation,[34] perhaps functioning as an ion transporter regulating intramelanosomal pH, which tightly regulates pigment production.[25,40] Lyst is involved in regulating organelle biogenesis and size and is mutated in Chediak–Higashi syndrome, where giant melano-

Table 1. Putative Stage-Related MNT1 Melanosomal Proteins of Special Interest[a]

UniProtKB accession no.	gene name	protein name	functional description
		Stage I (of 86)	
O14880	MGST3	Microsomal glutathione *S*-transferase 3	Glutathione *S*-transferase and glutathione peroxidase activities
O15533	TAPBP	Tapasin precursor (TPSN)	Involved in association of MHC-I with TAP and MHC peptide loading
P36955*	SERPINF1, PEDF	Pigment epithelium-derived factor precursor (PEDF)	Neurotrophic, induces neuronal differentiation; inhibitor of angiogenesis
Q14254	FLOT2	Flotillin-2 (Epidermal surface antigen)	Scaffolding protein, participating in formation of caveolae-like vesicles
Q16864	ATP6V1F	Vacuolar ATP synthase subunit F	Subunit of vacuolar ATPase essential for assembly or catalytic function, V-ATPase is responsible for acidic intracellular compartment
Q9HAQ7	PRP	ATP-binding cassette half-transporter	ABC transporter activity
		Stage II (of 131)	
P14415	ATP1B2	Sodium/potassium-transporting ATPase $\beta-2$ chain	Noncatalytic component of the active enzyme, which catalyzes the hydrolysis of ATP coupled with the Na^+ and K^+ ions exchange
P46459	NSF	Vesicle-fusing ATPase (*N*-ethylmaleimide sensitive fusion protein)	Required for vesicle-mediated transport, and transport from ER to Golgi; catalyzes fusion of transport vesicles within the Golgi cisternae
P53992	SEC24C	Protein transport protein Sec24C	Component of the COPII coat, that covers ER-derived vesicles involved in transport from the ER to the Golgi apparatus
Q04656	ATP7A	Copper-transporting ATPase 1	Supply copper to copper-requiring proteins within the secretory pathway, when localized in the trans-Golgi network
Q13277	STX3A	Syntaxin-3	Potentially involved in docking of synaptic vesicles
Q15036	SNX17	Sorting nexin-17	May be involved in several stages of intracellular trafficking
Q96A65	EXOC4	Exocyst complex component Sec8	Component of exocyst complex involved in docking of exocystic vesicles
Q9P0L0	VAPA	VAP-A, vesicle-associated membrane protein-associated protein A	Associate with SNARE and cytoskeleton proteins, may play a role in vesicle trafficking
		Stage IV (of 287)	
O00159	MYO1C	Myosin Ic	Myosins are actin-based motor molecules with ATPase activity and serving in intracellular movements
O94832	MYO1D	Myosin Id	
Q86T83	DKFZp451j0218	Hypothetical protein DKFZp451J0218	Nonmuscle myosin heavy chain, may have motor activity
Q16643	DBN1	Drebrin	May play some role in cell migration, extension of neuronal processes, and plasticity of dendrites, respectively. Binds F-actin
Q14847	LASP1	LIM and SH3 domain protein 1	Regulate dynamic actin-based, cytoskeletal activities. Agonist-dependent phosphorylation may regulate actin-associated ion transport
Q9H193	KIN13A	Kinesin-13A2	Microtubule-dependent motor protein involved in mannnose-6-phosphate receptor transport to the plasma membrane
P59998	ARPC4	Actin-related protein 2/3 complex subunit 4, ARPC4	Part of a complex implicated in the control of actin polymerization
P18206	VCL	Vinculin (Metavinculin)	Involved in cell adhesion. May be involved in the attachment of the actin-based microfilaments to the plasma membrane
Q13561	DCTN2	Dynactin subunit 2 (Dynactin complex 50 kDa subunit)	Modulates cytoplasmic dynein binding to an organelle, and plays a role in chromosome alignment and spindle organization during mitosis. May play a role in synapse formation during brain development
Q05682	CALD1	Caldesmon (CDM)	Actin- and myosin-binding protein implicated in the regulation of actomyosin interactions in smooth muscle and nonmuscle cells
P37802	TAGLN2	Transgelin-2 (SM22-α homologue)	Calponin-like, actin-, tropomyosin-, and calmodulin-binding protein believed to be involved in regulation or modulation of contraction
Q9H444	CHMP4B	VPS32	Component of ESCRT-III complex required for multivesicular bodies (MVBs) formation and sorting of endosomal cargo proteins into MVBs
*Q71RS6	SLC24A5	Sodium/potassium/calcium exchanger 5 precursor	Cation exchanger involved in pigmentation, probably transports 1 Ca^{2+} and 1 K^+ in exchange for 4 Na^+
P51810	GPR143	G-protein coupled receptor 143	Integrated membrane receptor, binds heterotrimeric G proteins
P45974	USP5	Ubiquitin thiolesterase 5	Cleaves linear and branched multiubiquitin polymers with a marked preference for branched polymers
Q96FW1	OTUB1	Ubiquitin thiolesterase protein OTUB1	Remove conjugated ubiquitin from proteins in vitro, may play regulatory role in preventing degradation. Regulator of T-cell anergy
P61088	UBE2N	Ubiquitin ligase	Catalyzes synthesis of noncanonical poly-ubiquitin chains. Mediates transcriptional activation and plays roles in cell cycle and DNA repair
Q8NE71	ABCF1	ATP-binding cassette sub-family F member 1	ATPase activity, may function in drug resistance

[a] Genes are listed that were found in only one stage of melanosome, as indicated. * = validated in this study.

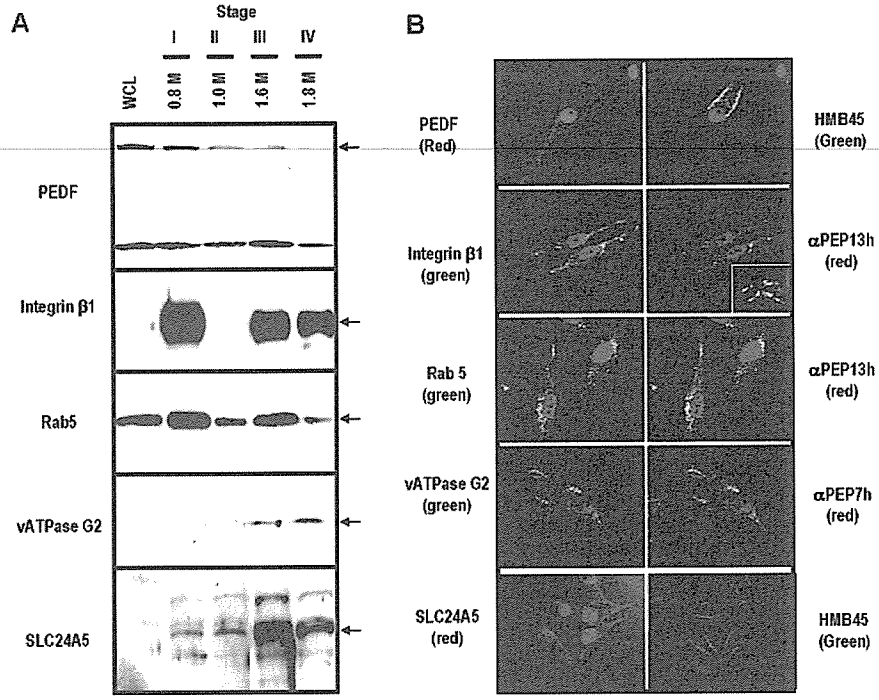

Figure 1. Validation of protein localization in melanosomes. (A) Confirmation of melanosome-identified proteins through antibody-specific detection in whole cell lysates (WCL) and melanosome fractions from MNT-1 melanoma cells using immunoblotting. (B) Dual immunofluorescence confocal microscopy confirmed the localization of proteins in melanosomes through comparison of the immunoreactivity patterns of polyclonal antibodies against PEDF,[29] SLC24A5, tyrosinase,[2] and Pmel17[17] (all in red) with reactivity patterns of monoclonal antibodies against integrin β1, RAB-5, vATPase, and HMB-45 (all in green). Differential interference contrast (DIC) images and nuclear counterstain with DAPI (blue) are included for visualization purposes.

somes, lysosomes, and platelet dense bodies are formed.[41] Matp is another transporter that regulates tyrosinase trafficking to melanosomes,[42] and mutations in that gene lead to a form of oculocutaneous albinism (type 4). Myo5a is part of the motor regulating melanosome transport to the periphery of melanocytes, a process essential to the distribution of melanosomes in the skin; mutations in Myo5a result in Griscelli syndrome.[43]

Mapping of Melanosome Proteins to Melanosomal Biogenic Pathways. To facilitate understanding of the dynamic process of melanosome biogenesis, the contribution of elements and complex membrane protein traffic input from several other organelles (e.g., the endoplasmic reticulum, early and late endosomes, and lysosomes) is illustrated, and the newly identified as well as known melanosome proteins are mapped to the melanosome biogenic pathways (Figure 2). The following five groups of proteins are depicted: (1) newly identified and validated in this study (e.g., PEDF and SLC24A5); (2) human homologues of mouse color genes identified in this study (e.g., Atp7a and MyoVa); (3) proposed stage-related proteins newly identified (e.g., Sec24 and vinculin); (4) proteins known as melanosome proteins from previous studies (e.g., Pmel17 and TYR); and (5) proteins common to other organelles (e.g., LAMP1). Many proteins detected in stage IV melanosomes are molecular motor- and cytoskeleton-related proteins, which may be necessary for directing fully pigmented melanosomes toward the cell periphery and their eventual transfer to keratinocytes. While it is obvious that multiple sources of cellular components contribute to the biogenesis of melanosomes, proteins more abundant in specific stages may define unique functions in that stage (e.g., the ion transporters VATPase and SLC24A5).

Discussion

Since the initial description of melanosome biogenesis by Seiji in 1963,[4] many research groups have attempted to further elucidate the synthesis and maturation of this organelle. The melanosome is an ideal model to study organelle biogenesis due to its characteristic maturation process and the fact that several specific markers are available.[5] Nevertheless, elucidating melanosome biogenesis has represented a formidable challenge due to the difficulty in isolating relatively short-lived early undifferentiated stage I melanosomes and in removing the melanin present in stage IV melanosomes. In this study, we took advantage of the fact that unpigmented SK-MEL-28 cells produce only stage I and II melanosomes and are thus a rich source of material. In addition, the enhanced combinations of sucrose density gradient purifications and an improved solubilization method, which allowed complete mass spectrometric analysis, provided information about melanosomal proteins at all stages of maturation. Many known integral membrane proteins were detected in late-stage melanosomes, such as those listed in Supplementary Table 2 (Supporting Information). However, full solubilization of hydrophobic membrane proteins in the presence of melanins is still difficult. The fact that some proteins were detected by LC/MS in early melanosomes but not in late melanosomes (or vice versa) may reflect

Table 2. Melanosomal Proteins Mapped to Mouse Coat Color[a]

gene symbol	murine locus	function in pigmentation	human melanosome protein (UniProtKB)	human disease (OMIM)
		Melanosome-Specific (Previously Identified)		
*DCT**	*slaty (slt)*	Tyrosinase-related protein 2 (TRP2)	**P40126:** L-dopachrome tautomerase precursor (EC 5.3.3.12)(DT)(DCT)	unknown
Gpr143	*Oa1 (oa1)*	Melanosome biogenesis signal transduction	**P51810**: G-protein coupled receptor143	Albinism, ocular, type I [300500]; Albinism, ocular, with late-onset sensorineural deafness (OASD) [300650]
si	*silver (si)*	melanosomal matrix protein	**P40967**: Melanocyte protein Pmel 17 precursor	Some oculocutaneous albinism? [155550]
Tyr	*albino, color (c)*	melanogenic enzyme	**P14679**: Tyrosinase precursor	OCA1 [203100]; OCA1B [606952]; WS2-OA [103470]
Tyrp1	*brown (b)*	melanosomal enzyme/stabilizing factor	**P17643**: 5,6-dihydroxyindole-2-carboxylic acid oxidase precursor.	Rufous albinism, ROCA [115501]; OCA3 [203290]; Precocious graying of hair [278400]
		Melanosome-Related (Previously Identified)		
Rab27a	*ashen (ash)*	melanosome transport	**P51159**: Ras-related protein Rab-27A	Griscelli syndrome, type 2 [607624]
Rab38	*chocolate (cht)*	Targeting of Tyrp1 protein to the melanosome	**P57729**: Ras-related protein Rab-38	unknown [606281]
		Melanosome-Newly Identified		
Atp7a	*mottled (mo)*	copper transport	**Q04656**: Copper-transporting ATPase 1	Menkes disease [309400]; Cutis laxa, X-linked [304150]
Ednrb	*piebald spotting (s)*	melanoblast differentiation	**P24530**: ET-B	Waardenburg-shah syndrome [277580]; Hirschsprung disease 2 (HSCR2) [600155]; Hirschsprung disease [142623]; ABCD syndrome [600501]
golden	*golden (gdn)*	Causes delayed and reduced development of melanin pigmentation	**Q71RS6:** Ion transporter JSX	Regulator of constitutive pigmentation
Gpnmb	*iris pigment dispersion (ipd)*	Apparent melanosomal component	**Q14956**: Transmembrane glycoprotein NMB precursor (Transmembrane glycoprotein HGFIN)	Glaucoma-related pigment dispersion syndrome-1 [604368]
Krt2−17	*dark skin 2 (Dsk2)*	Keratin	**P35908**: Keratin, type II cytoskeletal 2 epidermal	Ichthyosis, bullous type [146800]
Lyst	*beige (bg)*	Organelle biogenesis and size	**Q99698**: Lysosomal trafficking regulator	Chediak-Higashi syndrome; CHS [214500]
Matp	*underwhite (uw)*	transporter	**Q9UMX9**: Membrane-associated transporter protein, (SLC45A2)	OCA4 [606574]
Myo5a	*dilute (d)*	melanosome transport	**Q9Y4I1**:Myosin-5A	Griscelli syndrome, type 1; GS1214450; Elejalde syndrome 256710 Griscelli syndrome, type 3; GS3609227;
Ostm1	*grey-lethal (Gl)*	Pheomelanin and osteoclast function	**Q86WC4**: Osteopetrosis associated transmembrane protein 1 precursor	Osteopetrosis, autosomal recessive [259700]
Sfxn1	*flexed tail*	Tricarboxylate carrier	**Q9H9B4**: Sideroflexin-1	unknown

[a] The mouse coat color gene source: http://ifpcs.med.umn.edu/micemut.htm. *DCT was previously identified and validated as melanosome-specific proteins,[9] but is not present in current proteomic data sets.

limits to detection efficiency resulting from the relative amounts of proteins/peptides and the recovery from the digested sample.

Critical questions to address include which components are specific to melanosomes, and which may be critical to their maturation, transport, and/or transfer. Thus, unpigmented SK-MEL-28 cells express enzymes essential to melanogenesis, and comparisons of melanosomes from those cells with pigmented melanosomes from MNT1 cells identify a group of proteins involved in the regulation of melanin production. Another group of proteins identified in various melanosome stages may be involved in melanosome biogenesis, structure, and/or function. The presence of PEDF in early melanosomes had not been previously suspected. PEDF is a secreted factor important in melanoma tumor growth. Its presence in stage I melanosomes may be related to the common origin of this organelle with early endosomes, which transport this factor to the plasma membrane for secretion alone or encapsulated in exosomes.

In mammalian skin, melanosomes are transported toward the surface of melanocytes via microtubules. After their release from microtubules, melanosomes bind neighboring actin filaments at the cell periphery, where they are ultimately transferred to adjacent keratinocytes. Analysis of late-stage melanosomes reveals the presence of several molecular motors important for melanosome transport, such as kinesin, myosin Va, and dynein/dynactin, which are actively involved in mel-

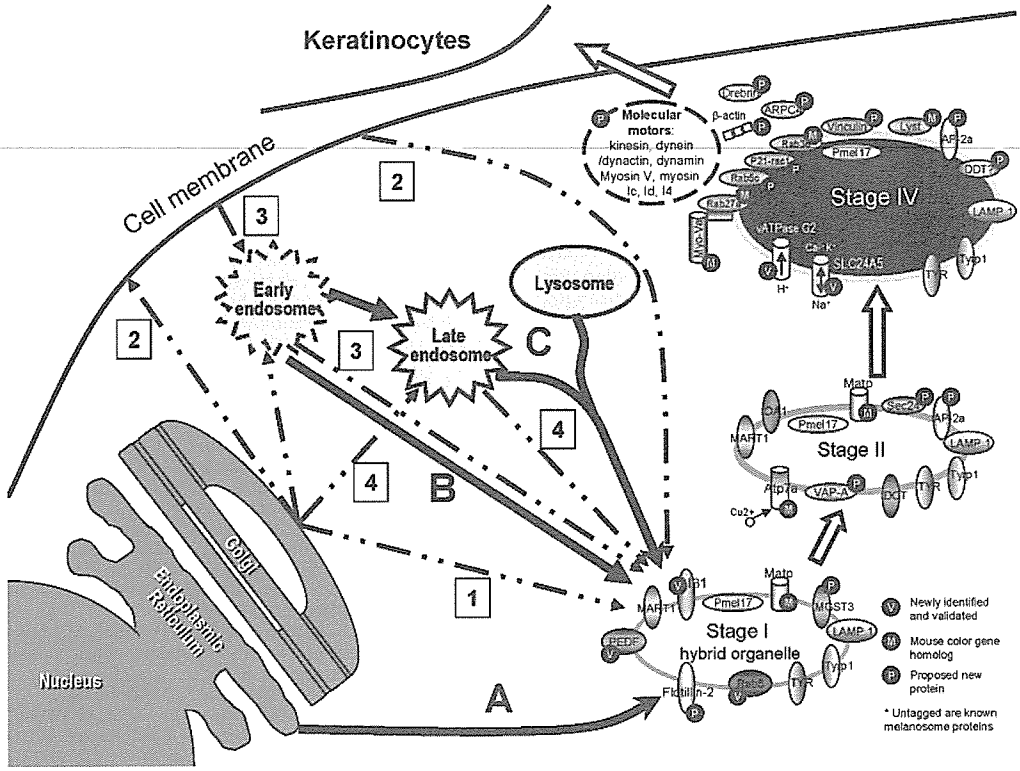

Figure 2. Overview of melanogenesis and protein sorting pathways as a dynamic source of proteins mapped in melanosomes (based on refs 17, 49, and 50). The melanosome proteome confirms the common origin of this organelle with other subcellular components, receiving elements (solid lines) from the endoplasmic reticulum (A), early endosomes (B), and from late endosomes or lysosomes (C). The dynamic nature of melanosomes is reflected in their complex membrane protein traffic (dashed lines) from Golgi (1), cell membrane (2), early endosomes (3), or late endosomes (4). Mature melanosomes are secreted to surrounding keratinocytes. Proteins of special interest related to each stage are depicted using oval (usually membrane-associated or cytosolic proteins) or cylinder shapes (usually known transmembrane proteins such as receptors or transporters). Proteins are tagged as V, newly identified and validated in this study; M, human homologous melanosome proteins of known mouse color genes, some known before and some newly identified in this study; and P, proposed stage-related proteins newly identified in this study. Known melanosomal and lysosomal proteins are not tagged (with V, M, or P).

anosome transport from melanocytes to keratinocytes. While they are not integral melanosomal proteins, they have important functions, such as melanophilin/Slac2-a, a binding protein involved in the transport of melanosomes via myosin Va.[44−46] In addition, several other organelle transport proteins were also detected in this study, such as dynamin, myosin Ic, myosin Id, and myosin I4. The roles of those proteins need to be examined in the future.

A number of proteins were exclusively detected in all stages of MNT1 melanosomes (which become pigmented) but were not present in SK-MEL-28 melanosomes (which remain amelanotic), indicating their potential importance in pigmentation. Melanosome-specific proteins directly involved in melanin synthesis, TYR and TYRP1, are primary examples, since they are expressed in nonpigmented cells but are not delivered to melanosomes, with the end result of disrupted pigmentation. Thus, the absence of TYR and TYRP1 in melanosomes from SK-MEL-28 cells (although they are expressed in those cells) is consistent with expectations.

Except for known melanosome proteins that give the organelle its unique structure and functions, a majority of proteins detected in the melanosome proteome are not organelle-specific. Some, such as ribosomal protein complexes, are obvious minor contaminants that were co-purified during sucrose gradient fractionation. Even though extra precaution was taken, sensitive mass spectrometers can always detect trace amounts of peptides that originate either from resident low-abundance proteins or from low-level contaminants. By searching our data against known human mitochondrial proteins annotated in UniProtKB, we estimate that the melanosome fractions at various stages are contaminated with mitochondrial proteins by <6% at early stage, and by <1−2% at late stage, indicating that our melanosome fractions are of high purity. On the other hand, many proteins identified in this study demonstrate that melanosomes are highly dynamic. They may be viewed as a microcosm of organelles, representing a dynamic balance of proteins as well as small molecules being transported in and out. Many of the "nonspecific" proteins might be associated with melanosomes only for a short period of time, or they may be proteins that reside in other subcellular compartments. In that sense, true permanent "resident" molecules for organelles may not exist.[47,48] Because of the uniqueness of melanosomes, a conventional negative control is not available for the analysis. Some of the most well-known endoplasmic reticulum, late endosomal, and lysosomal resident proteins have already proven to co-localize with melanosomes

and cannot be considered as contamination, although some proteins included in these datasets still need to be carefully evaluated and validated.

To explore the commonality between melanosomes and other organelles, we compared the melanosome proteome to partial proteomes of six other organelles currently available in the literature, including human neuromelanin granules, human platelets, human exosomes, rat synaptosomes, rat lysosomes, and mouse endoplasmic reticulum (human proteomes of the latter three organelles are not yet available). Interestingly, among all those six organelles, neuromelanin granules and exosomes have the highest percentage of proteins (60−75%) also found in melanosomes, while the other four have less than 50% of proteins common to melanosomes (data not shown). This comparison is consistent with the notion that neuromelanin granules are highly homologous to melanosomes. Melanocytes and neurons both derive from the neural crest, and the pigments in both types of organelles are derived similarly in the melanogenic and catecholamine pathways. This comparison also suggests a close relationship between the biogenesis of exosomes and melanosomes. This seems quite reasonable, given that both types of organelles are normally secreted from the host cells.

In summary, this multifaceted approach to understanding the makeup and biogenesis of melanosomes has not only revealed a large complement of constituent proteins, but has allowed many of them to be validated as components of melanosomes. Future work will examine the functions of those proteins in melanosomes and determine whether they play roles in regulating mammalian pigmentation, as well as further understand the biogenesis of lysosome-related organelles.

Acknowledgment. This research was supported by the Intramural Research Program of the NIH, National Cancer Institute, Center for Cancer Research, by USPHS Grants U01-HG02712 (NIH) and GM 37537 (D.F.H.), by NIH Grants HD40179 and RR01744, a Penn State Tobacco Settlement Grant, the Jake Gittlen Memorial Golf Tournament (K.C.C.), and by Indiana University Biomedical Research Support and IU Intercampus Research Funds (N.J.M.). We thank Prof. Hiroshi Shimizu of the Hokkaido University Graduate School of Medicine for his support of this study.

Supporting Information Available: Tables showing the melanosome proteins grouped into 12 subsets according to stage and cell type (Supplementary Table 1), common proteins identified in all stages of melanosomes (Supplementary Table 2), and Rab family members identified in stage I and stage II melanosomes (Supplementary Table 3). This material is available free of charge via the Internet at http://pubs.acs.org.

References

(1) Bennett, D. C.; Lamoreux, M. L. The color loci of mice—a genetic century. *Pigm. Cell Res.* **2003**, *16*, 333−344.
(2) Kushimoto, T.; Basrur, V.; Valencia, J. C.; Matsunaga, J.; Vieira, W. D.; Muller, J.; Appella, E.; Hearing, V. J. A new model for melanosome biogenesis based on the purification and mapping of early melanosomes. *Proc. Natl. Acad. Sci. U.S.A.* **2001**, *98*, 10698−10703.
(3) Basrur, V.; Yang, F.; Kushimoto, T.; Higashimoto, Y.; Yasumoto, K.; Valencia, J. C.; Muller, J.; Vieira, W. D.; Watabe, H.; Shabanowitz, J.; Hearing, V. J.; Hunt, D. F.; Appella, E. Proteomic analysis of early melanosomes: Identification of novel melanosomal proteins. *J. Proteome Res.* **2003**, *2*, 69−79.
(4) Seiji, M.; Shimao, K.; Birbeck, M. S. C.; Fitzpatrick, T. B. Subcellular localization of melanin biosynthesis. *Ann. N. Y. Acad. Sci.* **1963**, *100*, 497−533.
(5) Kushimoto, T.; Valencia, J. C.; Costin, G. E.; Toyofuku, K.; Watabe, H.; Yasumoto, K.; Rouzaud, F.; Vieira, W. D.; Hearing, V. J. The Seiji memorial lecture—The melanosome: an ideal model to study cellular differentiation. *Pigm. Cell Res.* **2003**, *16*, 237−244.
(6) Watabe, H.; Kushimoto, T.; Valencia, J. C.; Hearing, V. J. Isolation of melanosomes. *Curr. Protoc. Cell Biol.* **2005**, *Suppl. 26*, 3.14.1−3.14.15.
(7) Prota, G. Melanins, melanogenesis and melanocytes: looking at their functional significance from the chemist's viewpoint. *Pigm. Cell Res.* **2000**, *13*, 283−293.
(8) Wakamatsu, K.; Ito, S. Advanced chemical methods in melanin determination. *Pigm. Cell Res.* **2002**, *15*, 174−183.
(9) Ficarro, S. B.; McCleland, M. L.; Stukenberg, P. T.; Burke, D. J.; Ross, M. M.; Shabanowitz, J.; Hunt, D. F.; White, F. M. Phosphoproteome analysis by mass spectrometry and its application to *Saccharomyces cervisiae*. *Nat. Biotechnol.* **2002**, *20*, 301−305.
(10) Harris, M. A.; Clark, J.; Ireland, A.; Lomax, J.; Ashburner, M.; Foulger, R.; Eilbeck, K.; Lewis, S.; Marshall, B.; Mungall, C.; Richter, J.; Rubin, G. M.; Blake, J. A.; Bult, C.; Dolan, M.; Drabkin, H.; Eppig, J. T.; Hill, D. P.; Ni, L.; Ringwald, M.; Balakrishnan, R.; Cherry, J. M.; Christie, K. R.; Costanzo, M. C.; Dwight, S. S.; Engel, S.; Fisk, D. G.; Hirschman, J. E.; Hong, E. L.; Nash, R. S.; Sethuraman, A.; Theesfeld, C. L.; Botstein, D.; Dolinski, K.; Feierbach, B.; Berardini, T.; Mundodi, S.; Rhee, S. Y.; Apweiler, R.; Barrell, D.; Camon, E.; Dimmer, E.; Lee, V.; Chisholm, R.; Gaudet, P.; Kibbe, W.; Kishore, R.; Schwarz, E. M.; Sternberg, P.; Gwinn, M.; Hannick, L.; Wortman, J.; Berriman, M.; Wood, V.; de la, C. N.; Tonellato, P.; Jaiswal, P.; Seigfried, T.; White, R. The Gene Ontology (GO) database and informatics resource. *Nucleic Acids Res.* **2004**, *32*, D258−D261.
(11) Shevchenko, A.; Wilm, M.; Vorm, O.; Mann, M. Mass spectrometic sequencing of proteins silver-stained polyacrylamide gels. *Anal. Chem.* **1996**, *68*, 850−858.
(12) Ficarro, S. B.; McCleland, M. L.; Stukenberg, P. T.; Burke, D. J.; Ross, M. M.; Shabanowitz, J.; Hunt, D. F.; White, F. M. Phosphoproteome analysis by mass spectrometry and its application to *Saccharomyces cerevisiae*. *Nat. Biotechnol.* **2002**, *20*, 301−305.
(13) Coon, J. J.; Ueberheide, B.; Syka, J. E.; Dryhurst, D. D.; Ausio, J.; Shabanowitz, J.; Hunt, D. F. Protein identification using sequential ion/ion reactions and tandem mass spectrometry. *Proc. Natl. Acad. Sci. U.S.A.* **2005**, *102*, 9463−9468.
(14) Blonder, J.; Rodriguez-Galan, M. C.; Lucas, D. A.; Young, H. A.; Issaq, H. J.; Veenstra, T. D.; Conrads, T. P. Proteomic investigation of natural killer cell microsomes using gas-phase fractionation by mass spectrometry. *Biochim. Biophys. Acta* **2004**, *1698*, 87−95.
(15) Hu, Z. Z.; Valencia, J. C.; Huang, H.; Chi, A.; Shabanowitz, J.; Hearing, V. J.; Apella, E.; Wu, C. H. Comparative bioinformatics analyses and profiling of lysosome-related organelle proteomes. *Int. J. Mass Spectrom.* **2006**, in press.
(16) Wu, C. H.; Apweiler, R.; Bairoch, A.; Natale, D. A.; Barker, W. C.; Boeckmann, B.; Ferro, S.; Gasteiger, E.; Huang, H.; Lopez, R.; Magrane, M.; Martin, M. J.; Mazumder, R.; O'Donovan, C.; Redaschi, N.; Suzek, B. The Universal Protein Resource (UniProt): an expanding universe of protein information. *Nucleic Acids Res.* **2006**, *34*, D187−D191.
(17) Valencia, J. C.; Watabe, H.; Chi, A.; Rouzaud, F.; Chen, K. G.; Vieira, W. D.; Takahashi, K.; Yamaguchi, Y.; Berens, W.; Nagashima, K.; Shabanowitz, J.; Hunt, D. F.; Appella, E.; Hearing, V. J. Sorting of Pmel17 to melanocytes through the plasma membrane by AP1 and AP2: evidence for the polarized nature of melanocytes. *J. Cell Sci.* **2006**, *119*, 1080−1091.
(18) Han, D. K.; Eng, J.; Zhou, H.; Aebersold, R. Quantitative profiling of differentiation-induced microsomal proteins using isotope-coded affinity tags and mass spectrometry. *Nat. Biotechnol.* **2001**, *19*, 946−951.
(19) Washburn, M. P.; Wolters, D.; Yates, J. R., III. Large-scale analysis of the yeast proteome by multidimensional protein identification technology. *Nat. Biotechnol.* **2001**, *19*, 242−247.
(20) Blonder, J.; Goshe, M. B.; Moore, R. J.; Pasa-Tolic, L.; Masselon, C. D.; Lipton, M. S.; Smith, R. D. Enrichment of integral membrane proteins for proteomic analysis using liquid chromatography-tandem mass spectrometry. *J. Proteome Res.* **2002**, *1*, 351−360.
(21) Szpoganicz, B.; Gidanian, S.; Kong, P.; Farmer, P. Metal binding by melanins: studies of colloidal dihydroxyindole-melanin, and its complexation by Cu(II) and Zn(II) ions. *J. Inorg. Biochem.* **2002**, *89*, 45−53.
(22) Liu, Y.; Simon, J. D. Metal-ion interactions and the structural organization of Sepia eumelanin. *Pigm. Cell Res.* **2005**, *18*, 42−48.

(23) Samokhvalov, A.; Liu, Y.; Simon, J. D. Characterization of the Fe(III)-binding site in Sepia eumelanin by resonance Raman confocal microspectroscopy. *Photochem. Photobiol.* **2004**, *80*, 84−88.
(24) Fuller, B. B.; Spaulding, D. T.; Smith, D. R. Regulation of the catalytic activity of preexisting tyrosinase in Black and Caucasian human melanocyte cell cultures. *Exp. Cell Res.* **2001**, *262*, 197−208.
(25) Watabe, H.; Valencia, J. C.; Yasumoto, K.; Kushimoto, T.; Ando, H.; Muller, J.; Vieira, W. D.; Mizoguchi, M.; Appella, E.; Hearing, V. J. Regulation of tyrosinase processing and trafficking by organellar pH and by proteasome activity. *J. Biol. Chem.* **2004**, *279*, 7971−7981.
(26) Ramakrishna, V.; Treml, J. F.; Vitale, L.; Connolly, J. E.; O'Neill, T.; Smith, P. A.; Jones, C. L.; He, L. Z.; Goldstein, J.; Wallace, P. K.; Keler, T.; Endres, M. J. Mannose receptor targeting of tumor antigen pmel17 to human dendritic cells directs anti-melanoma T cell responses via multiple HLA molecules. *J. Immunol.* **2004**, *172*, 2845−2852.
(27) Skipper, J. C.; Gulden, P. H.; Hendrickson, R. C.; Harthun, N.; Caldwell, J. A.; Shabanowitz, J.; Engelhard, V. H.; Hunt, D. F.; Slingluff, C. L., Jr. Mass-spectrometric evaluation of HLA-A*0201-associated peptides identifies dominant naturally processed forms of CTL epitopes from MART-1 and gp100. *Int. J. Cancer* **1999**, *82*, 669−677.
(28) Kawakami, Y.; Robbins, P. F.; Wang, R. F.; Parkhurst, M. R.; Kang, X.; Rosenberg, S. A. The use of melanosomal protein in the immunotherapy of melanoma. *J. Immunother.* **1998**, *21*, 237−246.
(29) Abe, R.; Shimizu, T.; Yamagishi, S.; Shibaki, A.; Amano, S.; Inagaki, Y.; Watanabe, H.; Sugawara, H.; Nakamura, H.; Takeuchi, M.; Imaizumi, T.; Shimizu, H. Overexpression of pigment epithelium-derived factor decreases angiogenesis and inhibits the growth of human malignant melanoma cells in vivo. *Am. J. Pathol.* **2004**, *164*, 1225−1232.
(30) Zhu, N.; Lalla, R.; Eves, P.; Brown, T. L.; King, A.; Kemp, E. H.; Haycock, J. W.; Macneil, S. Melanoma cell migration is upregulated by tumour necrosis factor-alpha and suppressed by alpha-melanocyte-stimulating hormone. *Br. J. Cancer* **2004**, *90*, 1457−1463.
(31) Brakebusch, C.; Fassler, R. beta 1 integrin function in vivo: adhesion, migration and more. *Cancer Metastasis Rev.* **2005**, *24*, 403−411.
(32) Simpson, J. C.; Jones, A. T. Early endocytic Rabs: functional prediction to functional characterization. *Biochem. Soc. Symp.* **2005**, 99−108.
(33) Raposo, G.; Tenza, D.; Murphy, D. M.; Berson, J. F.; Marks, M. S. Distinct protein sorting and localization to premelanosomes, melanosomes and lysosomes in pigmented melanocytic cells. *J. Cell Biol.* **2001**, *152*, 809−823.
(34) Lamason, R. L.; Mohideen, M. A.; Mest, J. R.; Wong, A. C.; Norton, H. L.; Aros, M. C.; Jurynec, M. J.; Mao, X.; Humphreville, V. R.; Humbert, J. E.; Sinha, S.; Moore, J. L.; Jagadeeswaran, P.; Zhao, W.; Ning, G.; Makalowska, I.; McKeigue, P. M.; O'Donnell, D.; Kittles, R.; Parra, E. J.; Mangini, N. J.; Grunwald, D. J.; Shriver, M. D.; Canfield, V. A.; Cheng, K. C. SLC24A5, a putative cation exchanger, affects pigmentation in zebrafish and humans. *Science* **2005**, *310*, 1782−1786.
(35) Toyofuku, K.; Wada, I.; Spritz, R. A.; Hearing, V. J. The molecular basis of oculocutaneous albinism type 1 (OCA1): sorting failure and degradation of mutant tyrosinase results in a lack of pigmentation. *Biochem. J.* **2001**, *355*, 259−269.
(36) Toyofuku, K.; Wada, I.; Valencia, J. C.; Kushimoto, T.; Ferrans, V. J.; Hearing, V. J. Oculocutaneous albinism (OCA) types 1 and 3 are ER retention diseases: mutations in tyrosinase and/or Tyrp1 influence the maturation, degradation of calnexin association of the other. *FASEB J.* **2001**, *15*, 2149−2161.
(37) Bahadoran, P.; Aberdam, E.; Mantoux, F.; Bille, K.; Busca, R.; Yalman, N.; de Saint Basile, G.; Casaroli, R.; Ortonne, J. P.; Ballotti, R. Rab27a: a key to melanosome transport in human melanocytes. *J. Cell Biol.* **2001**, *152*, 843−849.
(38) Loftus, S. K.; Larson, D. M.; Baxter, L. L.; Antonellis, A.; Chen, Y.; Wu, X.; Jiang, Y.; Bittner, M.; Hammer, J. A.; Pavan, W. J. Mutation of melanosome protein Rab38 in *chocolate* mice. *Proc. Natl. Acad. Sci. U.S.A.* **2002**, *99*, 4471−4476.
(39) Spritz, R. A.; Ho, L.; Furumura, M.; Hearing, V. J. Mutational analysis of copper-binding by human tyrosinase. *J. Invest. Dermatol.* **1997**, *109*, 207−212.
(40) Smith, D. R.; Spaulding, D. T.; Glenn, H. M.; Fuller, B. B. The relationship between Na(+)/H(+) exchanger expression and tyrosinase activity in human melanocytes. *Exp. Cell Res.* **2004**, *298*, 521−534.
(41) Huizing, M.; Anikster, Y.; Gahl, W. A. Hermansky-Pudlak syndrome and Chediak-Higashi syndrome: disorders of vesicle formation and trafficking. *Thromb. Haemostasis* **2001**, *86*, 233−245.
(42) Costin, G. E.; Valencia, J. C.; Vieira, W. D.; Lamoreux, M. L.; Hearing, V. J. Tyrosinase processing and intracellular trafficking is disrupted in mouse primary melanocytes carrying the uw mutation: a model for oculocutaneous albinism (OCA) type 4. *J. Cell Sci.* **2003**, *116*, 3203−3212.
(43) Spritz, R. A. Multi-organellar disorders of pigmentation: tied up in traffic. *Clin. Genet.* **1999**, *55*, 309−317.
(44) Fukuda, M.; Kuroda, T. S.; Mikoshiba, K. Slac2-a/melanophilin, the missing link between Rab27 and myosin Va. *J. Biol. Chem.* **2002**, *277*, 12432−12436.
(45) Westbroek, W.; Lambert, J.; De Schepper, S.; Kleta, R.; Van Den, B. K.; Seabra, M. C.; Huizing, M.; Mommaas, M.; Naeyaert, J. M. Rab27b is up-regulated in human Griscelli syndrome type II melanocytes and linked to the actin cytoskeleton via exon F-Myosin Va transcripts. *Pigm. Cell Res.* **2004**, *17*, 498−505.
(46) Wu, X.; Tsan, G. L.; Hammer, J. A. Melanophilin and myosin Va track the microtubule plus end on EB1. *J. Cell Biol.* **2005**, *171*, 201−207.
(47) Brunet, S.; Thibault, P.; Gagnon, E.; Kearney, P.; Bergeron, J. J.; Desjardins, M. Organelle proteomics: looking at less to see more. *Trends Cell Biol.* **2003**, *13*, 629−638.
(48) Huber, L. A.; Pfaller, K.; Vietor, I. Organelle proteomics: implications for subcellular fractionation in proteomics. *Circ. Res.* **2003**, *92*, 962−968.
(49) Hearing, V. J. Biogenesis of pigment granules: a sensitive way to regulate melanocyte function. *J. Dermatol. Sci.* **2005**, *37*, 3−14.
(50) Luzio, J. P.; Poupon, V.; Lindsay, M. R.; Mullock, B. M.; Piper, R. C.; Pryor, P. R. Membrane dynamics and the biogenesis of lysosomes. *Mol. Membr. Biol.* **2003**, *20*, 141−154.

PR060363J

Clinical dermatology • **Concise report**

doi: 10.1111/j.1365-2230.2005.01974.x

Two cases of folliculosebaceous cystic hamartoma

S. Tanimura, K. Arita, F. Iwao, M. Kasai, Y. Fujita, H. Kawasaki, R. Abe, D. Sawamura, T. Kimura* and H. Shimizu

*Department of Dermatology, Hokkaido University Graduate School of Medicine, Sapporo, Japan; and *Sapporo Institute for Dermatopathology, Sapporo, Japan*

Summary

Folliculosebaceous cystic hamartoma (FSCH) is a rare cutaneous hamartoma composed of dilated folliculosebaceous units associated with mesenchymal elements. Two cases of FSCH with typical histopathological features are reported. Patient 1 was a 60-year-old man presented with a normal skin-coloured asymptomatic nodule on his scalp. Patient 2 was a 70-year-old man with an asymptomatic nodule on his right auricle that had persisted for the previous 15 years. In all, 34 cases of FSCH have been reported in the English literature. Clinically, the lesions are asymptomatic, usually rubbery to firm in consistency, and usually occur on or above the neck (> 90%). Most lesions do not exceed 25 mm in diameter (> 90%). Histopathologically, FSCH shares several similar features to sebaceous trichofolliculoma, but it is usually possible to differentiate these two tumours.

Introduction

Folliculosebaceous cystic hamartoma (FSCH) is widely considered to be a hamartoma composed of multiple tissue elements, including both ectodermal and mesodermal components. Epithelial components comprise adnexal and folliculosebaceous cystic proliferations, while mesenchymal components exhibit variable fibroplasias with vascular and adipose tissue. Here, we report two cases of FSCH with typical histopathological features.

Case reports

Patient 1

A 60-year-old man presented with a tumour on his scalp, which had become apparent some 10 years previously. Physical examination showed a normal skin-coloured, elastic soft asymptomatic nodule, 25 mm in diameter, with a smooth surface covering of skin (Fig. 1a). Histopathological examination (Fig. 1b, c) revealed a markedly dilated follicular cystic structure lined by stratified squamous epithelium. Abundant, mature, sebaceous lobules radiated outward from the cystic structure. The cysts showed a predominant infundibular keratinization pattern, and were surrounded by a dense fibrovascular stroma with mucin deposition. These features were characteristic of FSCH.

Patient 2

A 70-year-old man visited our clinic for an asymptomatic nodule on the right auricle that had persisted for 15 years. The lesion was a normal skin-coloured pedunculated soft nodule, 10 mm in diameter (Fig. 2a). We made an initial clinical diagnosis of the lesion as a soft fibroma and excised it completely. Histopathologically, a dilated follicular cystic structure was observed (Fig. 2b,c), with numerous sebaceous lobules arising from its wall in the dermis and subcutis. There were excess fibrous components around these structures, with adipocyte hyperplasia, small venules and sweat

Correspondence: Dr Shintaro Tanimura, Department of Dermatology, Hokkaido University Graduate School of Medicine, N 15, W 7, Sapporo 060-8638, Japan.
E-mail: shintaro-g500@jcom.home.ne.jp

Conflict of interest: none declared.

Accepted for publication 28 June 2005

